

Review

Perfluoropyridine: Discovery, Chemistry, and Applications in Polymers and Material Science

Ritesh Gautam ¹, Ian Geniza ¹, Scott T. Iacono ¹ , Chadron M. Friesen ²  and Abby R. Jennings ^{1,*}

¹ Department of Chemistry, United States Air Force Academy, Colorado Springs, CO 80840, USA; c22ritesh.gautam@afacademy.af.edu (R.G.); c23ian.geniza@afacademy.af.edu (I.G.); scott.iacono@afacademy.af.edu (S.T.I.)

² Department of Chemistry, Trinity Western University, 22500 University Drive, Langley, BC V2Y 1Y1, Canada; chad.friesen@twu.ca

* Correspondence: abby.jennings@afacademy.af.edu

Abstract: Perfluoropyridine (PFPy) is an organofluorine compound that has been employed for a variety of applications, from straightforward chemical synthesis to more advanced functions, such as fluorinated networks and polymers. This can be directly attributed to the highly reactive nature of PFPy, especially towards nucleophilic aromatic substitution (SNAr). The aim of this review is to highlight the discovery and synthesis of PFPy, discuss its reactive nature towards SNAr, and to summarize known reports of the utilization and thermal analysis of PFPy containing fluoropolymers and fluorinated network materials.

Keywords: perfluoropyridine; nucleophilic aromatic substitution; fluoropolymers; organofluorine



Citation: Gautam, R.; Geniza, I.; Iacono, S.T.; Friesen, C.M.; Jennings, A.R. Perfluoropyridine: Discovery, Chemistry, and Applications in Polymers and Material Science. *Molecules* **2022**, *27*, 1616. <https://doi.org/10.3390/molecules27051616>

Academic Editor: Renzo Luisi

Received: 4 February 2022

Accepted: 25 February 2022

Published: 28 February 2022

Publisher's Note: MDPI stays neutral with regard to jurisdictional claims in published maps and institutional affiliations.



Copyright: © 2022 by the authors. Licensee MDPI, Basel, Switzerland. This article is an open access article distributed under the terms and conditions of the Creative Commons Attribution (CC BY) license (<https://creativecommons.org/licenses/by/4.0/>).

1. Introduction

The fluorine atom exhibits many unique properties, including a small atomic radius, large electronegativity, and minimal polarizability [1]. Thus, when coupled with carbon in the form of a C-F bond, organofluorine compounds with highly sought after properties can be obtained [2]. Many of these fluorinated compounds display increased hydrophobicity, as well as enhanced chemical and oxidative resistance, and improved thermal stability [3]. Accordingly, organofluorine compounds have found applications in a range of areas, such as medical imaging [4,5], pharmaceuticals [6], and agrochemicals [7]. Furthermore, driven by the growing demand to develop novel high-performance materials, fluorinated compounds are often used as the building blocks of more complex chemical systems, such as fluoropolymers and fluorinated network materials [8].

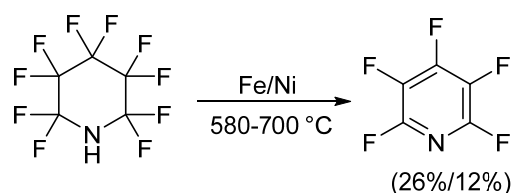
There are a number of different organofluorine compounds that have been used as starting materials for more complex systems and polymers. Organofluorine compounds used for these materials can be derived directly from a commercially sourced fluorinated starting material or prepared in-house using selective or direct fluorination techniques [9–11]. The motivation for choosing one feedstock over another weighs heavily on the overall synthetic demand of the polymer or material, scalability, cost, and desired properties. With the growing variety of commercially available fluorinated starting materials, often times, researchers will utilize commercial sources versus turning to the more synthetically demanding routes of direct fluorination.

Perfluoropyridine, or PFPy, is one example of these fluorinated compounds that has been used for a wide variety of purposes, ranging from general synthetic reactions [12,13] to complex pharmaceuticals [14–16] and materials [17–19]. Although it can be prepared in house by employing the methods described below, PFPy is commercially available, and is considered to be an economically viable option in modern times. Furthermore, as discussed in the subsequent sections, PFPy is a very reactive molecule and can be used to develop more complex fluorinated starting materials. The goal of the present review is to highlight

the history and synthetic routes used to obtain PFPy, provide an overview of its unique reactivity, and demonstrate its use in preparing fluorinated networks and polymers.

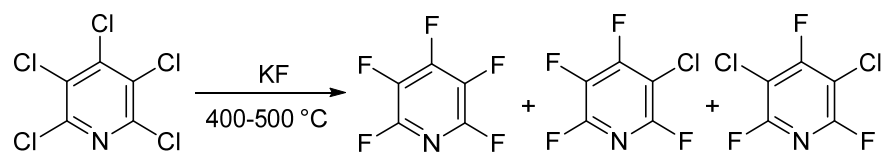
2. Discovery and Synthesis of Perfluoropyridine

The first reported synthetic methods for obtaining PFPy occurred in the early 1960s and involved defluorination of perfluoropiperidine [20–23]. In these instances, perfluoropiperidine, which was synthesized electrochemically from pyridine and anhydrous hydrogen fluoride [24], was passed over a metal, either iron or nickel, at high temperatures. PFPy was then isolated through chromatographic methods. When iron was implemented, PFPy was obtained at a 26% yield. A slightly lower recovery, 12%, was found when defluorination was conducted using nickel (Scheme 1) [20–22].



Scheme 1. Synthesis of PFPy from perfluoropiperidine.

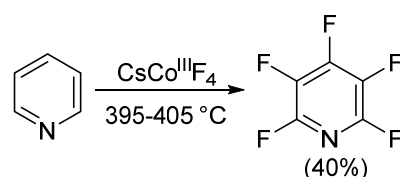
In 1964 and 1965, two different groups—Chambers et al. [25–27] and Banks et al. [28,29]—published similar methods for the synthesis of PFPy. Here, the authors were able to prepare PFPy by heating pentachloropyridine in an autoclave with anhydrous potassium fluoride. Pentachloropyridine was prepared by reacting pyridine with phosphorous pentachloride [30]. In this instance, a mixture of products was obtained but could be separated by distillation (Scheme 2) [25–29].



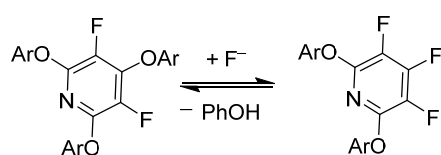
Scheme 2. Synthesis of PFPy using anhydrous potassium fluoride.

The total amount of halogenated products was about 90%, and the ratio of products could be tuned by changing the temperature and reaction time. Under optimal conditions, PFPy could be obtained at a yield of 83% [29]. The method shown in Scheme 2 is still the gold standard for synthesizing PFPy commercially.

Since the development of the commercial method for obtaining PFPy in the mid-1960s, little progress on obtaining PFPy by other means has been made. Nearly 20 years later, Banks et al. obtained trace quantities of PFPy by co-pyrolyzing pentafluoro(trichloromethyl) benzene and 4-(dichloroamino)tetrafluoropyridine under nitrogen [31]. The same year, Coe and Sleigh pyrolyzed a number of pyrrolidines in the presence of iron [32]. This reaction produced a mixture of products, and similar to the report by Banks [31], PFPy was obtained in very low quantities (<12%). Later, in 1982, Plevey and co-workers were able to obtain PFPy at a yield of 40% by fluorinating pyridine with cesium tetrafluorocobalate (III) [33]. Despite this, they were also met with challenges and encountered a point of diminishing returns on the yield when the reaction was attempted above a 5 g scale (Scheme 3) [33].

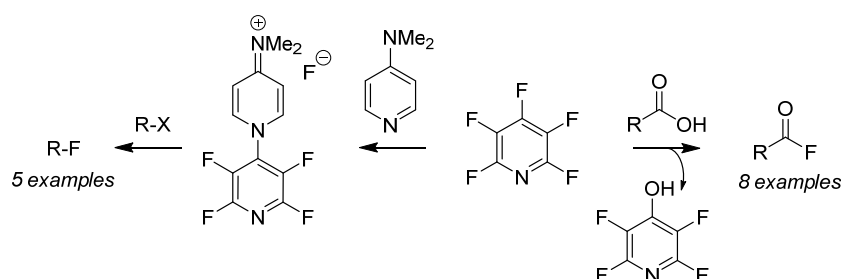


Scheme 3. Synthesis of PFPy using cesium tetrafluorocobalate (III).



Scheme 5. PFPy and its reversibility to complex products with phenols.

Perfluoropyridine has been employed as a nucleophilic fluorination reagent for both alkyl halides (Scheme 6, *right-to-left*) [46] as well as deoxyfluorination of carboxylic acids (Scheme 6, *left-to-right*) [47] for the preparation of a versatile pool of substrates. Fluorination of organo-halides (R-X) is achieved after generation of the air-stable fluoride salt from the addition of PFPy and dimethylaminopyridine [46]. Furthermore, the in situ generation of acyl fluorides is readily accomplished by the nucleophilic addition of carboxylic acids with PFPy [47]. The ester intermediate then undergoes cleavage from unsequestered fluoride, producing phenol as a by-product and the desired acyl fluoride. This strategy was expanded to include the ‘one-pot’ preparation of amides and esters utilizing PFPy as a coupling agent.



Scheme 6. PFPy as a nucleophilic fluorinating agent.

The last examples of purposeful manipulation of PFPy involve site selective defluorination and halogen exchange (halex), as illustrated in Scheme 7 [48,49]. Both processes generate a regioselective substitution depending on various reaction conditions. Senaweera et al. demonstrated high photocatalytic turnover with low-Ir complex loading for the preparation of dehydrofluorinated PFPy utilizing a flow reactor design, demonstrating the scalability of such useful intermediates [48]. The halex reverse-substitution was achieved in the 4-*para*-position of PFPy with LiCl, and additional exchanges on the ring with chlorine were achieved from a combination of kinetic and thermodynamic control [49].



Scheme 7. PFPy as a scaffold for selective hydrodefluorination.

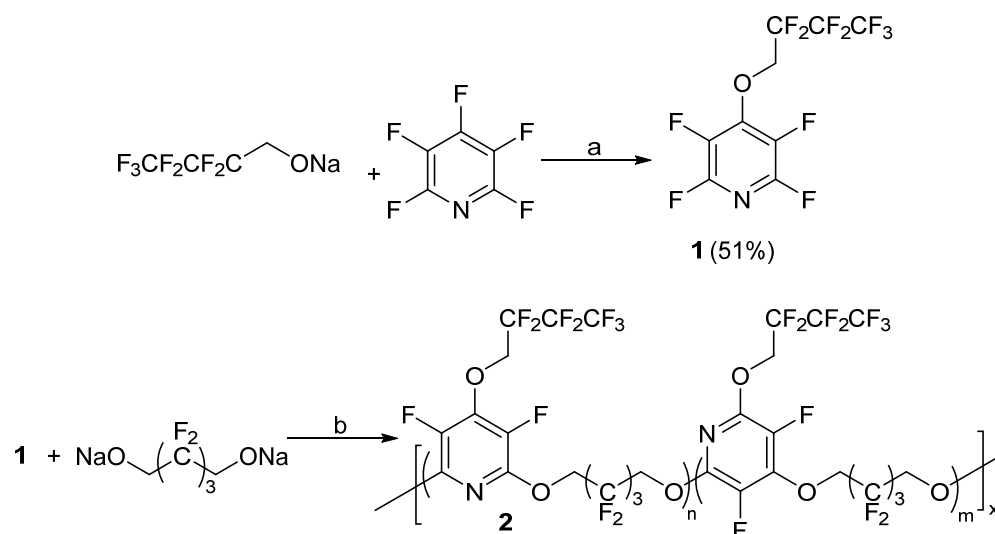
4. Perfluoropyridine Used in Polymers and Materials

Since Teflon’s serendipitous discovery in 1938 by Roy J. Plunkett [50], the search for new fluorinated polymers and materials has continued. There are a considerable number of peer-reviewed reports highlighting this unique class of materials, their highly sought after properties, and advanced applications. In fact, just within the last five years alone, over 100 review articles and book chapters have been published on the topic of fluorinated materials and polymers [35]. The driving force for this is the continued demand for new and improved materials for advanced applications. Adding to the properties observed with simple organofluorine compounds, fluoropolymers and materials are also endowed with having low dielectric constants, refractive indexes, surface energy, flammability, and water absorptivity [51]. Furthermore, these materials are often more mechanically durable and morphologically diverse [52]. With such robust attributes, this unique class of materials

has found use in a variety of specialized areas including the aerospace and automotive industries, advanced surfaces and coatings, medical devices, structural components, and many more [53,54].

Synthetic methods to obtain fluoropolymers and networks vary widely. As with simple organofluorine molecules, a fluoropolymer or fluorinated material can be achieved by direct fluorination methods [55] or by using a fluorinated monomer or building block [11]. With PFPy's unique and high reactivity, it has been utilized in both routes—to fluorinate an existing polymer or material and to prepare more diverse fluorinated building blocks. The use of PFPy in fluorinated networks and polymers will be discussed below.

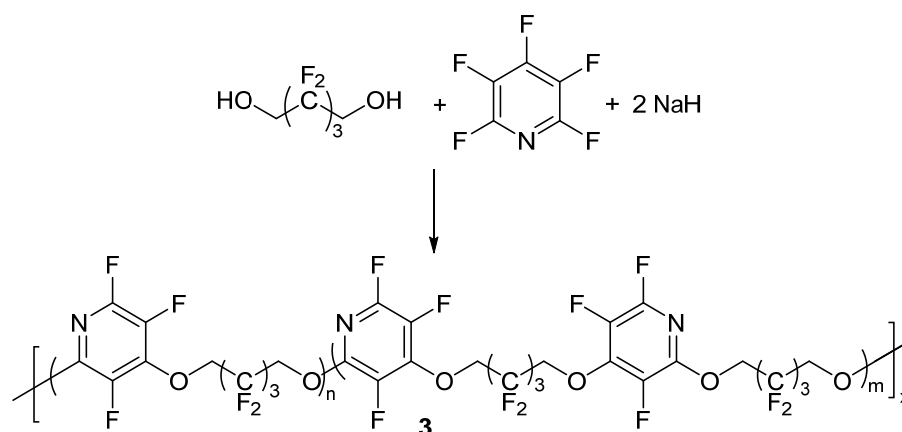
One of the first known reports of using PFPy for the synthesis of polymeric materials was presented in the late 1970s by Johncock, Hewins, and Cunliffe [56]. With the implementation of PFPy in the polymers, the authors' objective was to obtain fluoropolymers that exhibited enhanced structural and oxidative stability, low glass transition temperatures (T_g s), and elastomeric properties, making the fluoropolymers appropriate materials for applications in the aerospace industry. With the knowledge that PFPy is reactive towards nucleophilic substitution and that it exhibits bifunctionality, the authors employed the Williamson Ether synthetic method to prepare new PFPy-based fluoropolymers. In one example, the authors initially reacted PFPy with the sodium salt of 2,2,3,3,4,4,4-heptafluoro-1-butanol to obtain a polymeric precursor, **1**. Precursor **1** was further reacted with the sodium salt of 2,2,3,3,4,4-hexafluoro-1,5-pentandiol to obtain a PFPy-based polymer (**2**, Scheme 8) [56].



Scheme 8. Synthesis of polymeric precursor **1** and homo/copolymer **2**. Conditions: a = DMF, 15 °C for 30 min then 45 °C for 1 h; b = THF/TMS, 15 °C for 1 h then 50 °C for 3.5 h.

Upon purification of the sample by solvent fractionation and characterization by ^{19}F NMR, the authors determined that the fluoropolymer obtained was a mixture of a homopolymer ($n = 0, m = 1$), which was the result of the expected nucleophilic addition at 4-position, and copolymer ($n/m = 2$), which was the result of the nucleophilic substitution reaction in the 4-position and the competing displacement reaction between the fluorinated butoxy group and the fluorine atoms in the 2- and 6-positions [57].

In another example, the authors also prepared a different copolymer by reacting the sodium salt of 2,2,3,3,4,4-hexafluoro-1,5-pentandiol with PFPy (Scheme 9) [56]. Under these conditions, the authors were able to obtain about 70% soluble polymer and roughly 6% of an insoluble gel. The gel was believed to be a network which resulted from the tri-substitution of the PFPy ring. The polymer fraction was isolated by solvent displacement.



Scheme 9. Synthesis of copolymer **3**. Conditions: THF/TMS, 5 °C for 2 h, RT for 16 h, then 50 °C for 5 h.

The copolymer structure of **3** was determined by ^{19}F NMR. Since the nucleophilic substitution of PFPy is more favorable at the 4-position than the 2 or 6-position [58,59], the authors concluded, that intermediates **4** and **5** (Figure 1) will likely form first. Intermediates **4** and **5** would then serve as the main building blocks of the fluoropolymer and support the structure of **3** [56].

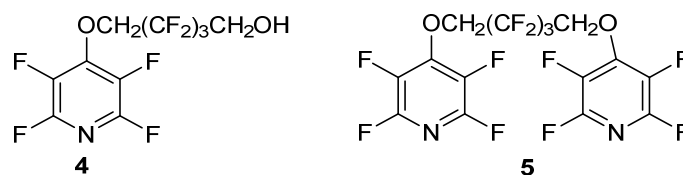


Figure 1. PFPy intermediates formed in the preparation of copolymer **3**.

The polymers shown in Schemes 8 and 9 were also characterized by differential scanning calorimetry (DSC), thermogravimetric analysis (TGA), and their viscosities were determined. Table 2 summarizes the data collected for **2** and **3** [56].

Table 2. Characterization data obtained for **2** and **3** [56]¹.

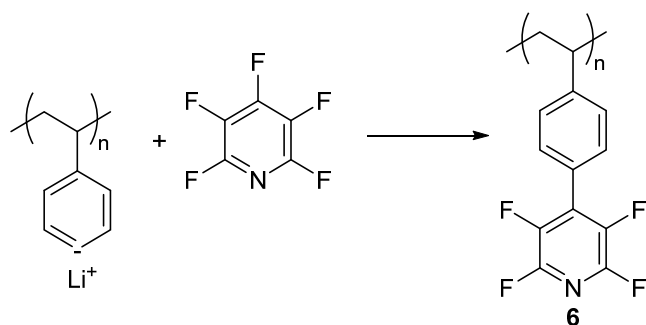
Polymer	η_{inh} (dL/g)	T_g (°C)	T_d (°C, O ₂ /Air)
2 ($n/m \sim 2$)	0.10	2	265/330
3 ($n/m \sim 2$)	0.50	−5	300/350
3 ($n/m \sim 2$)	0.22	−12 ²	300/360
3 ($n = 0, m = 1$)	0.19	−10	310/350

¹ When data for more than one sample are given, samples are from different experiments.² At 20 °C/min.

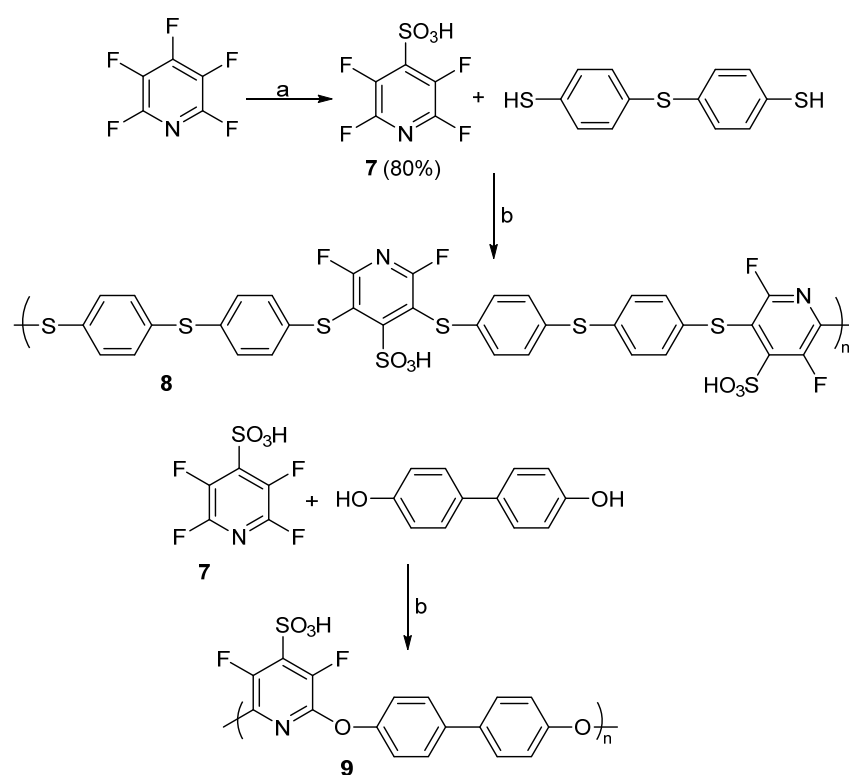
About 10 years later, the next known study of using PFPy in a polymer was reported by Banks and Tsiliopoulos [60]. In their example, the authors initially brominated and then lithiated linear polystyrene. The lithiated polystyrene was then reacted with PFPy to yield **6** (Scheme 10) [60]. Polymer **6** was fully fluorinated by treatment with F_2/N_2 . No experimental or characterization data were provided for **6**, or the final, fully fluorinated material. This is the first study where PFPy is employed as a pendant group on the polymer vs. the backbone of the polymer/network. The PFPy was also not included in the original monomer but incorporated as the pendant group, post-polymerization.

In a later study by Seyb and Kerres, the authors used PFPy to prepare sulfonated poly(arylene ethers) for potential applications in proton exchange membranes (PEMs) [61]. Initially, compound **7** was prepared by the nucleophilic thiolation of PFPy, followed by oxidation of the thiol to sulfonic acid. Next, **7** was reacted with 4,4'-thiobisbenzenethiol or 4,4'-dihydroxybiphenol to obtain a new poly(arylene thioether) or poly(arylene ether),

respectively (**8** or **9**, Scheme 11) [61]. Characterization of polymer **8** and **9** by ^{19}F NMR analysis indicated the structures shown.



Scheme 10. Synthesis of polymer **6**.



Scheme 11. Synthesis of poly(arylene thioether) **8** and poly(arylene ether) **9**. Conditions: a = NaSH/H₂O₂ then HCOOH/H₂O₂; b = DMAc, 2 equiv. K₂CO₃, 100 °C for 24 h.

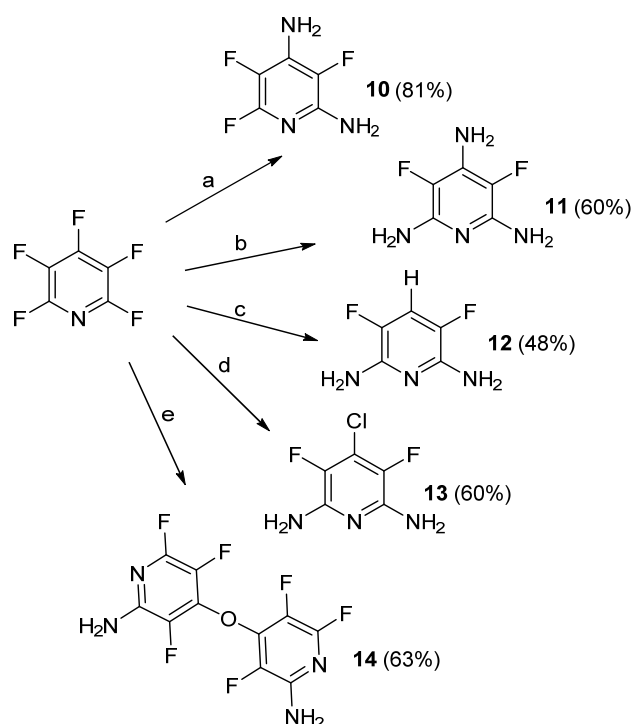
GPC analysis was used to determine the number average molecular weight (M_n), weighted average molecular weight (M_w), and dispersity (D) of **8** and **9**. Once characterized, the authors blended the polymers shown with polybenzimidazole (PBI)-Celazol[®] in order to obtain PEMs that could be utilized in polymer electrolyte fuel cells. By incorporating **8** or **9** into the blend, the authors hoped to enhance the thermal stability and chemical resistance of the membrane towards H₃PO₄. Characterization of the polymers and blends by TGA-FTIR demonstrated that the onset of degradation for the sulfonic acid groups ($T_{\text{SO}_3\text{H}}$) ranged between 328 and 419 °C, whereas the degradation of the polymer backbone (T_{backbone}) ranged between 332 and 461 °C. Additionally, **9** and its corresponding blend were more thermally stable than the **8** and its blend. Overall, the blends were more thermally stable than the polymers alone. In terms of oxidative stability, as determined by Fenton's test, the authors concluded that future work to obtain higher molecular weight polymers was needed to fully optimize this parameter. The conductivity of the blends

was also tested and compared to Nafion[®]. The films were stable up to 180 °C and also outperformed Nafion[®]. The results from the analyses performed by Seyb and Kerres are summarized in Table 3 [61].

Table 3. Data obtained by Seyb and Kerres [61].

Polymer/Blend	M_n (kDa)	M_w (kDa)	D	T_{SO_3H} (°C)	$T_{backbone}$ (°C)	σ (S/cm)
8	12.5	30	2.39	328	332	
9	5.9	10.2	1.74	378	366	
8/PBI-Celazol [®]				359	461	0.04
9/PBI-Celazol [®]				419	410	0.02

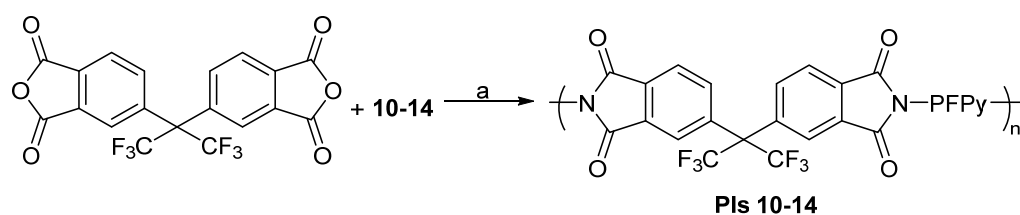
Between 2007 and 2013, Vaganova et al. utilized PFPy to make a number of fluorinated pyridylenediamine monomers (**10–14**, Scheme 12) [62–64].



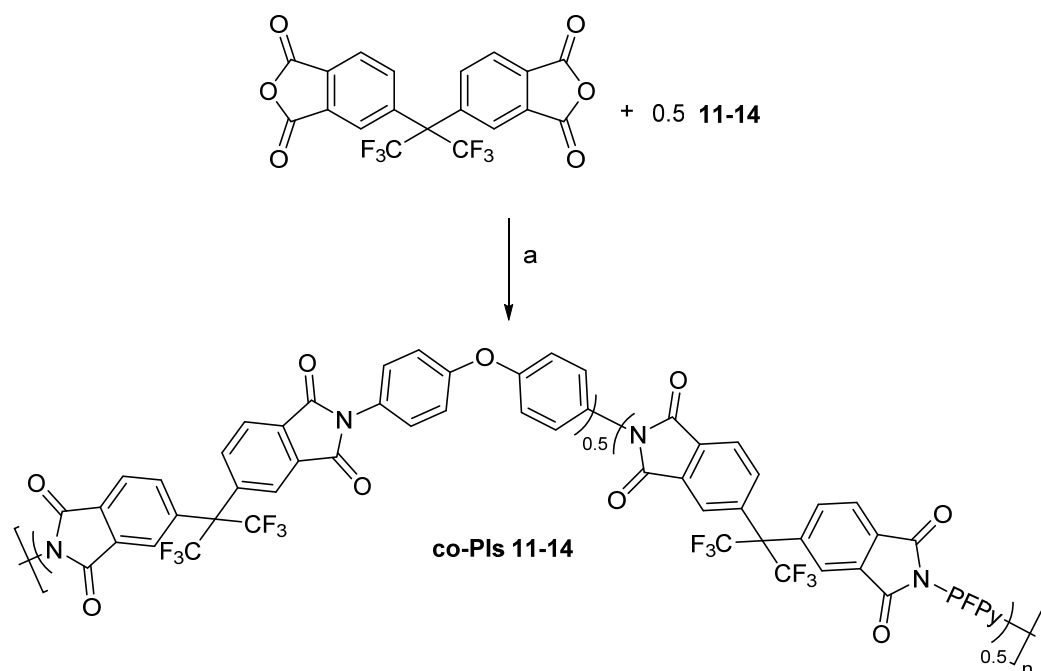
Scheme 12. Fluorinated pyridylenediamine monomers prepared by Vaganova et al. Conditions: a = NH₃ (ex), 100 °C, 15 h; b = NH₃ (ex), 150 °C, 50 h; c = 1.1 equiv. Zn, 1.7 equiv. NaOH, H₂O, 20 °C, 10 h, then NH₃ (ex), 120 °C, 35 h; d = 1.5 equiv. CaCl₂, dicyclohexano-18-crown-6, sulfolane, reflux, 5 h, then NH₃ (ex), 110 °C, 10 h; e = tetrafluoro-4-pyridinoxide, sulfolane, reflux, 20 h, then NH₃ (ex), 10–15 °C, 10 h.

These monomers were then used in a later study to prepare fluorinated polyimides (PIs) and co-polyimides (co-PIs), using one-step polycondensation reactions. The polymers were prepared for potential applications as materials for carbonized membranes [64]. For the PIs, a stepped heating was used and all polymerizations were carried out in benzoic acid (BA) melts (Scheme 13) [64]. The number average molecular weights of the PIs were determined by ¹⁹F NMR.

Similarly, the co-PIs were prepared from monomers **11–14** and 4,4'-oxydianiline in order to obtain higher molecular weight polymers that exhibit enhanced mechanical properties (Scheme 14) [63]. The molecular weights were not determined for the co-PIs, but the authors concluded that they had higher molecular weights than the PIs because these materials had increased viscosities.



Scheme 13. PIs prepared from fluorinated pyridylenediamine monomers, **10–14**. Conditions: a = stepped heating, BA melt.



Scheme 14. Co-PIs prepared from fluorinated pyridylenediamine monomers, **10–14**. Conditions: a = 140 °C, BA melt, then 0.5 equiv. oxydianiline, BA melt.

The PIs and co-PIs were thermally and thermo-oxidatively characterized using DSC and TGA analysis. The T_g s of the PIs were found to be higher than the co-PIs. The lower T_g s obtained for the co-PIs were attributed to the increased flexibility of the polymers as a result of the incorporation of 4,4'-oxydianiline. The polymeric materials demonstrated good thermal and oxidative stabilities, with most having $T_{5\%} \geq 500$ °C. Table 4 summarizes some of the characterization data obtained by Vaganova et al. [64]. Mechanical testing was performed using dynamic mechanical analysis (DMA) on films prepared from the co-PIs. These materials retained their storage modulus up to their T_g s. The authors concluded that the co-PI films had good thermomechanical properties as a result of the 4,4'-oxydianiline; however, the PIs were not analyzed by DMA.

The PIs were pyrolyzed under inert conditions and the chemical composition was analyzed at various temperatures in order to evaluate the polymers' potential for use in carbonized materials. It was determined that the PIs underwent a selective and consecutive elimination of the different heteroatoms contained within and this could be utilized to tailor the properties of the nanostructured carbonized membranes formed from PIs **10–14** [64].

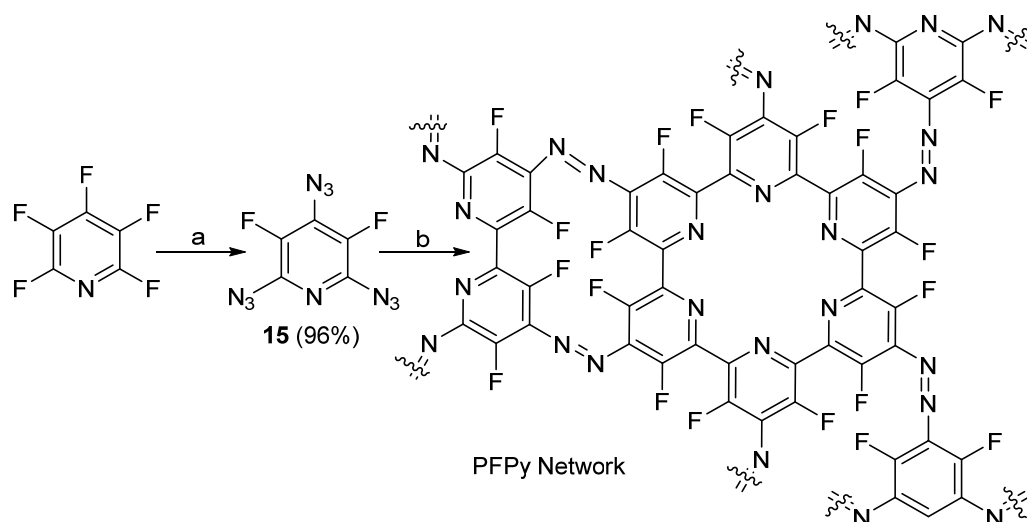
In 2018, Nedel'ko et al. synthesized 3,5-difluoro-2-4-6-triazidopyridine using a previously published method, which involved the SNAr of PFPy with sodium azide [65]. The authors then studied the thermal decomposition of **15** using DSC. The degradation products were also characterized using IR spectroscopy [66]. Comparing the IR spectra of the degradation products of **15** with previously studied compounds (2,4,6-triazidopyridine, 2,4,6-triazidopyrimidine, and cyanuric triazide), the authors determined that because **15** lacks hydrogen atoms, its degradation mechanism favors the formation of a network of

planar polyconjugated carbon–nitrogen porphyrin-like structures as a result of a complex chain polymerization (Scheme 15) [66].

Table 4. Selected data obtained by Vaganova et al. [64].

PI/co-PI	M_n (kDa)	η_{inh} (dL/g)	T_g (°C)	$T_{5\%}^1$ (°C)	$T_{5\%}^2$ (°C)
PI 10	14.5	0.09	345	515	493
PI 11	17.5	-	347	519	491
PI 12	30.5	0.18	346	519	503
PI 13	12.0	0.14	344	504	500
PI 14	22.5	0.17	315	432	430
co-PI 11	ND	0.45	300	526	513
co-PI 12	ND	0.42	288	525	495
co-PI 13	ND	0.35	284	522	507
co-PI 14	ND	0.28	294	465	480

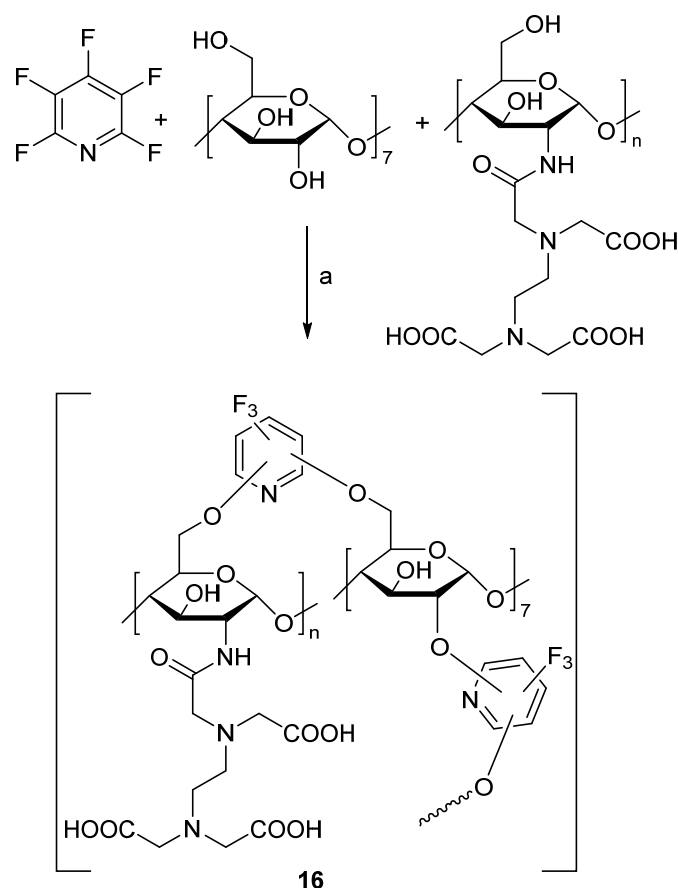
¹ Temperature at 5% weight loss under He. ² Temperature at 5% weight loss under a 80:20 He:O₂ mixture.



Scheme 15. Thermal decomposition of 2,4,6-triazido-3,5-difluoropyridine, **15**. Conditions: a = DMSO, 3.2 equiv. NaN₃, RT, 10 h; b = 160–172 °C.

Additionally, in 2018, Yu and co-workers utilized PFPy to prepare porous β -cyclodextrin (β -CD) polymers for use in the removal of heavy metals and organic pollutants from water [67]. In their study, the authors utilized PFPy to join EDTA-modified chitosan with β -CD (or cellulose, sodium alginate, and alkali lignin) through the SNAr reaction of the hydroxyl groups of the biomolecules (Scheme 16) [67].

The resulting polymer, **16**, was characterized by FT-IR and solid state ¹³C NMR spectroscopy, which confirmed the incorporation of PFPy with the EDTA-modified chitosan and β -CD polymers. Further characterization by Brunauer–Emmett–Teller (BET) surface area analysis and scanning electron microscopy (SEM) indicated that **16** was porous and had a specific surface area of 47.8 m²/g, making it a promising material for an adsorbent. Energy dispersive X-ray analysis showed that **16** contained both nitrogen and fluorine, supporting the results observed by FT-IR and solid state ¹³C NMR spectroscopy. Adsorption studies were conducted with **16** and Pb (II), Ni (II), Cu (II), bisphenol A, trichlorophenol, and 6-bromo-2-naphthol. The polymer was found to remove the contaminants with over 91% efficiency, whereas a sample consisting of cross-linked β -CD polymer only had a 40% efficiency under comparable conditions. Furthermore, **16** was found to be recyclable and, after five cycles, still maintained over 91% adsorption capacity [67].

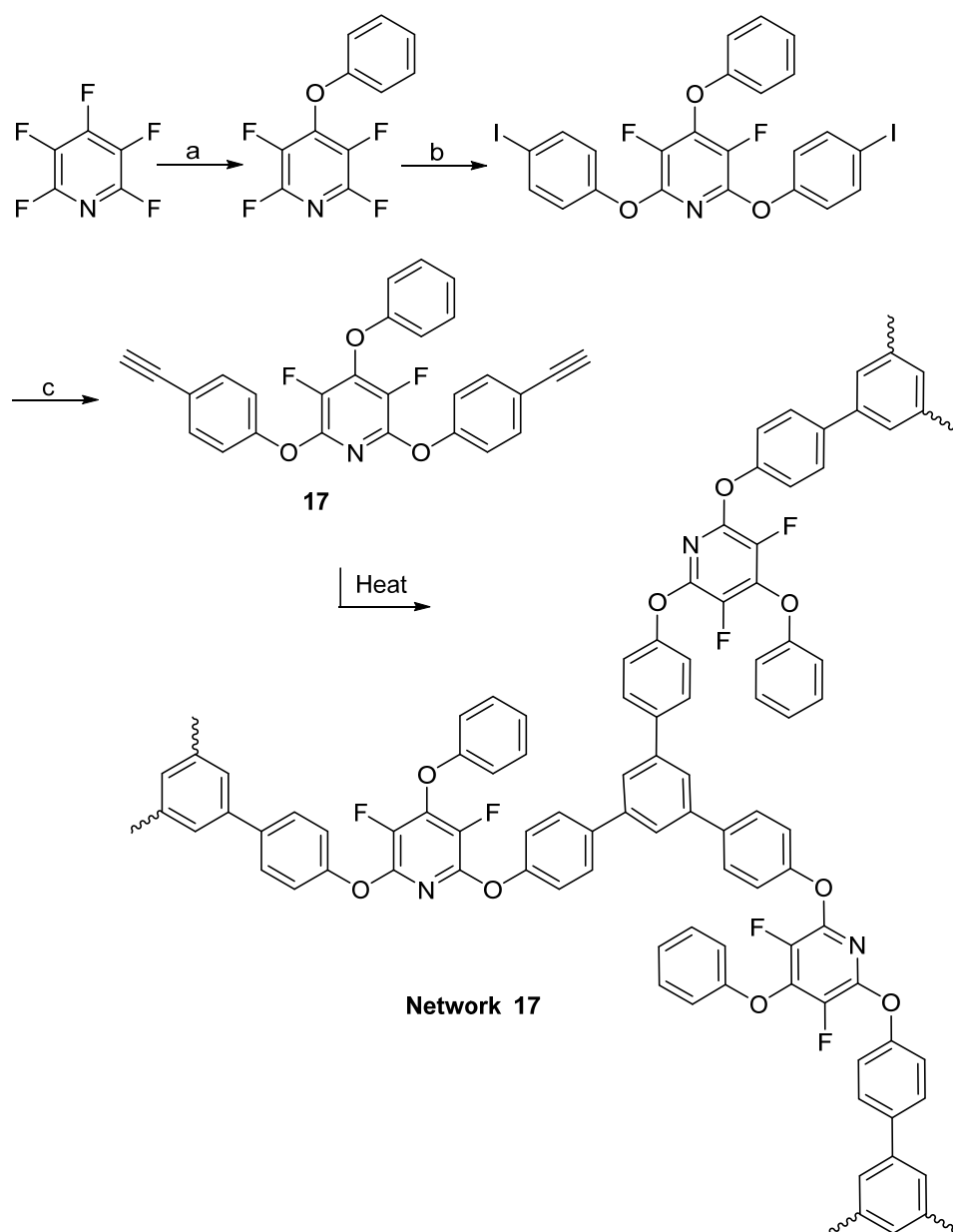


Scheme 16. Synthesis of PFPy-functionalized porous β -CD polymers. Conditions: a = MeTHF:H₂O, K₂CO₃, 80 °C, 48 h.

In 2019, Corley et al. demonstrated [2 + 2 + 2] cyclopolymerizations of 2,6-bis(4-ethynylphenoxy)-3,5-difluoro-4-aryloxy pyridine (**17**) for thermoset resins having intractable polyarylene networks [68]. All the polymeric products communicated in their work were derived from commercially sourced feed stocks of PFPy and functionalized phenols. To synthesize **17**, oxygen-based nucleophiles go through a selective S_NAr reaction with PFPy specifically at the 4-position using potassium carbonate. The additions at the 2 and 6-positions onto PFPy are then favorable with 4-iodo-phenol when using cesium carbonate in DMF. To complete the monomer (**17**), palladium and copper iodide are used to couple an ethyne onto the aromatic ring, by way of interacting TMS-ethyne with the iodo-bond on the aromatic ring. Thermal analysis indicated crosslinking of the monomer to form Network **17** (Scheme 17) [68].

Further cycloadditions were also considered and demonstrated. For example, 1,3-dipolar alkyne-azide “click” cycloaddition reactions were accomplished with the reaction of **17** with mono- or bis-(azidomethyl) benzene, generating a variety of polytriazole polymers (Figure 2) [68].

In all cases, these network materials showed excellent temperature resistance. The 2 + 2 + 2 cycloaddition networks exhibited thermal decomposition onset at 450 °C. The slow, near-linear weight loss of 45 wt% from 500 °C to 1000 °C (0.9 wt% °C⁻¹) under nitrogen is indicative of a highly dense network of carbonaceous material. A 20 wt% glassy carbon char was evident at 1000 °C. For the “click” cycloaddition polymer, the onset of degradation at 300 °C with linear decomposition to a glassy carbon char yield of 10 wt% is typical for polytriazoles with molecular weights between 2000 and 8000 g/mol. The authors also suggested that the high thermal stability indicated that the cycloadditions did not compromise the fluorinate pyridine core repeat unit [68].



Scheme 17. Preparation and network formation of **17**. Conditions: a = ArOH, DMF, K_2CO_3 , RT, 16 h; b = 4-I-PhOH, Cs_2CO_3 , DMF, 45 min; c = Pd/CuI, ethynyltrimethylsilane, and then TBAF.

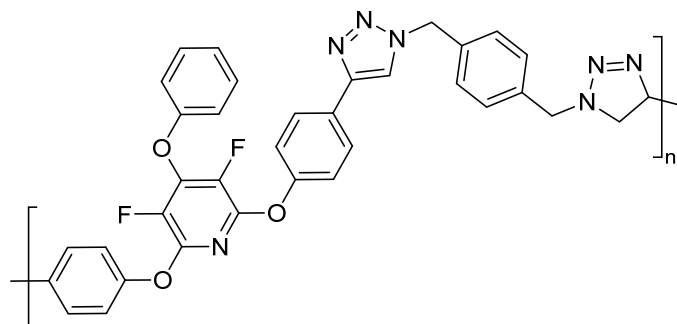
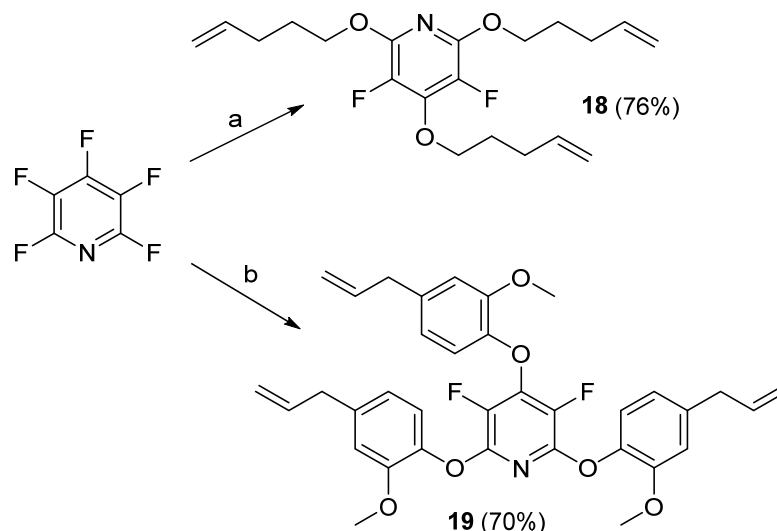


Figure 2. Polymer prepared from the cycloaddition of **17**. Conditions: DCM, 4-bis(azidomethyl)benzene, CuI, HOAc, DPEA, RT, 24 h.

In early 2020, Moore and co-workers prepared a new class of semifluorinated thiol-ene thermoset materials that were explored as aerospace sealants and coatings [69]. In this study, the authors developed two new trisubstituted alkene monomers, **18** and **19**, by reacting 4-penten-1-ol and eugenol with PFPy (Scheme 18) [69].



Scheme 18. Synthesis of monomers **18** and **19**. Conditions: a = 4-penten-1-ol, DMF, Cs_2CO_3 , 65 °C, 24 h; b = eugenol, DMF, Cs_2CO_3 , 65 °C, 24 h.

Thiol-ene thermoset materials were synthesized using 3,6-dioxa-1,8-octanedithiol (ODT) and trimethylolpropane tris(mercaptopropionate) (TMPMP) and the newly targeted alkene monomers. Formulations were mixed at a 1:1 thiol:ene ratio, with 1 wt% of 2,2-dimethoxy-2-phenylacetophenone (DMPA) as the UV photo-initiator (Figure 3) [69].

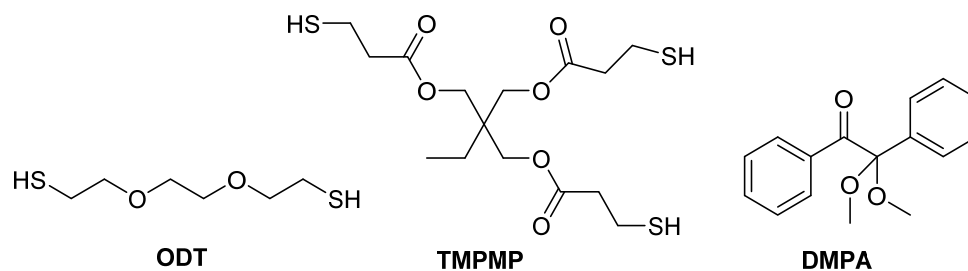


Figure 3. Multifunctional thiols and photo-initiator utilized to make thiol-ene thermosets.

The resulting polymeric systems based on these novel monomers demonstrated T_g s ranging from -42 to 21 °C. The use of the trifunctional thiol results in a higher T_g (i.e., TMPMP). Thermal degradation temperatures at 5% mass loss ($T_{d,5\%}$) spanned from 274 to 348 °C in nitrogen and char yields varied from 13.2 to 28.7% (see Table 5) [69].

This new class of semifluorinated thermoset materials with their measured properties have several potential applications within the aerospace industry, such as sealants and coatings, where stability and survivability at high temperatures in harsh environmental conditions are imperative [69].

At around the same time, Houck et al. reported the synthesis of two highly soluble high aromatic content (HAC) perfluoropyridine-based thermosetting precursors [70]. Previously, to obtain polymers or materials that contain HAC, transition-metal-catalyzed coupling or harsh fluorination methods were required. However, utilizing the reactivity of PFPy towards SNAr , Houck et al. readily obtain monomers **22** and **23** in moderate yields. Initially, regioselective nucleophilic addition takes place with PFPy by first reacting it with lithiated 1,2-diphenylethyne or anthracene at the 4-position, to generate compounds **20**

and **21**, respectively. To complete the monomers, further reactions are accomplished at both the 2 and 6-position by lithiated 1,2-diphenylethyne to generate monomers **22** and **23**, respectively (Scheme 19) [70].

Table 5. Selected thermal data obtained by Moore and co-workers [69].

System ¹	T_g (°C)	Predicted T_g ² (°C)	$T_{d,5\%}$ (°C)	Char Yield (%)
18			143	0
19			259	7.5
ODT				
100:0	−42	-	274	13.2
75:25	−29	−28	279	17.8
50:50	−15	−16	289	21.7
25:75	−3	−6	296	23.3
0:100	3	-	325	23.2
TMPMP				
100:0	−17	-	275	13.2
75:25	1	−5	280	18.8
50:50	10	5	288	23.5
25:75	19	14	305	23.5
0:100	21	-	348	28.7

¹ Ratios given are mol ratios of **18:19** used in the thiol-ene network with either ODT or TMPMP, respectively.

² Predicted T_g value obtained from the Fox equation.

Upon curing **22** and **23** at 341 and 372 °C (T_{max}), respectively, both systems yielded insoluble cross-linked networks. The cured network of **22** displayed an onset of decomposition (T_d) of 470 °C and a char yield of 51% at 900 °C, while the cured network of **23** displayed a T_d of 456 °C and a char yield of 81% at 900 °C (Table 6) [70].

The ease of thermal setting, combined with the formation of rigid cross-linked networks of highly densified polyarylenes exhibiting high decomposition temperatures and high char yields indicate these thermoset polymers are promising templates for nanomaterials in microelectronics and for use in high-temperature applications in the aerospace industry [70].

In mid-2020, Eismeier and co-workers employed PFPy to prepare step-growth polymers and networks [71]. To prepare the step-growth polymers, compound **24** was prepared by SNAr reaction of PFPy with phenylmagnesium bromide [72]. This was then reacted with bisphenol A (BPA) to obtain the step-growth polymer, **24** (Scheme 20) [71]. ¹⁹F NMR indicated successful nucleophilic addition and formation of the desired polymer. End group analysis of **25** by ¹H NMR indicated a molecular weight of 4000 g/mol.

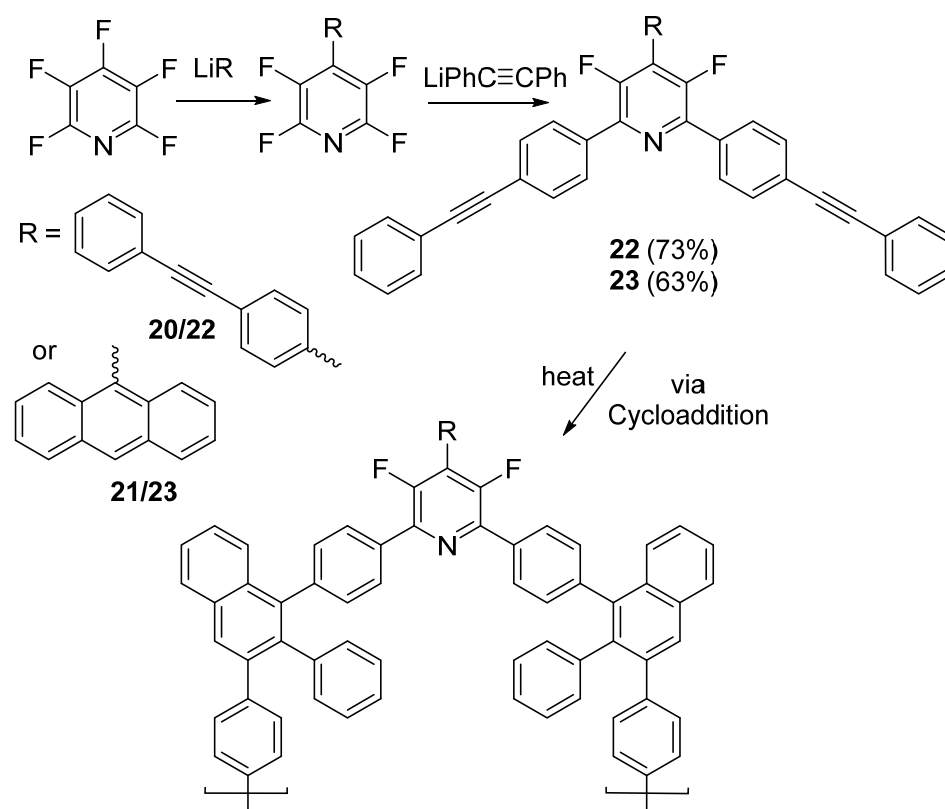
Table 6. Selected thermal data obtained by Houck et al. [70].

Entry	T_m (°C)	T_{onset} (°C)	T_{max} (°C)	T_d Ar/Air (°C)	Char Yield ¹ Ar/Air (%)
22	93, 108	306	341	470/480	51/2
23	-	327	372	456/483	81/1

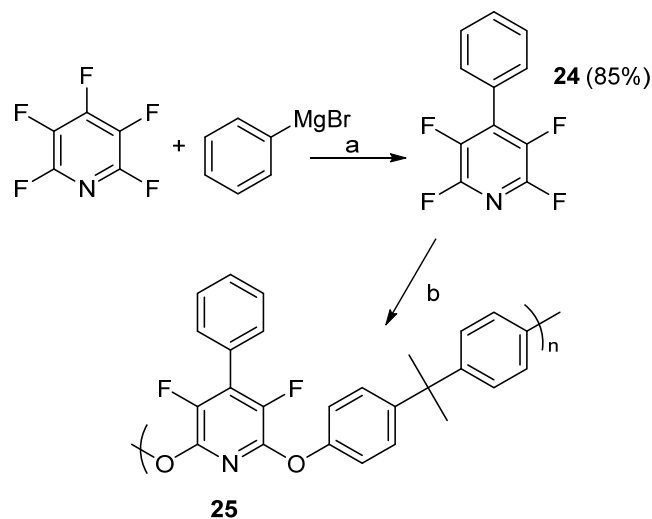
¹ Determined at 900 °C.

Additionally, PFPy was reacted using similar conditions with 1,3,5-benzenetrimethanol or phloroglucinol to prepare fluorinated network materials, **26** and **27**, respectively (Scheme 21) [71].

Networks **26** and **27** were thermally characterized by DSC and TGA. The results from these studies are summarized in Table 7. The TGA analysis was performed under argon. Given the char yield of the networks and chemical composition of the materials, **25–27** could find potential applications for resins in the aerospace industry, low surface energy materials, and low dielectric constant materials [71].



Scheme 19. Synthesis and network formation of **22** and **23**.

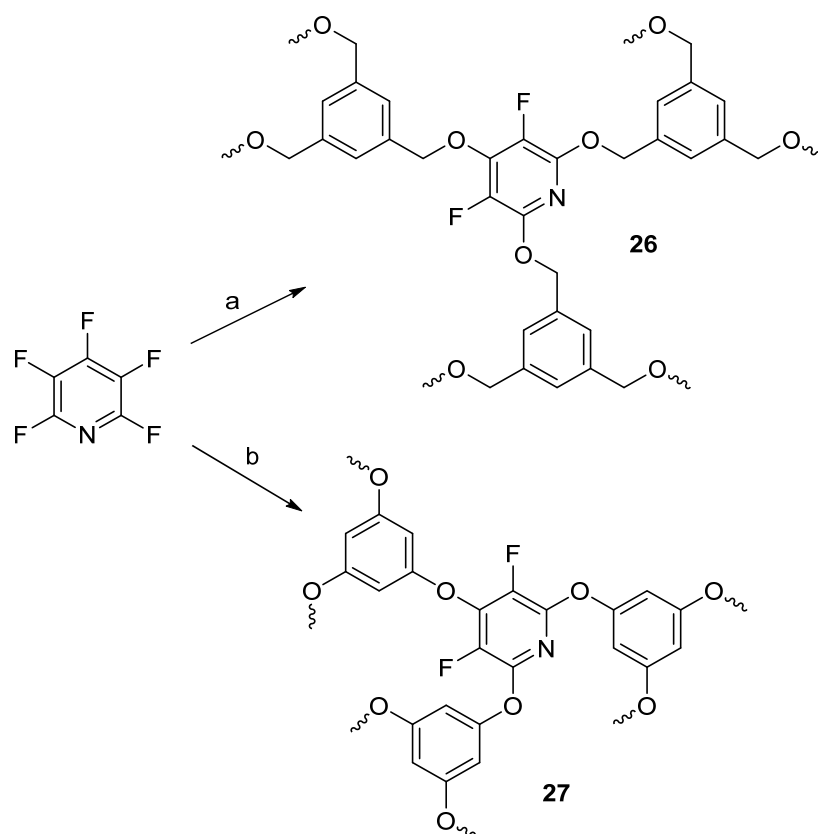


Scheme 20. Step-growth polymers prepared from compound **24**. Conditions: a = THF, RT, 24 h; b = DMF, bisphenol-A, 0.3 equiv. NaH, 65 °C, 16 h.

Table 7. Selected thermal data obtained by Eismeier and co-workers [71].

Network	T_g ¹ (°C)	T_d ² (°C)	Char Yield ² (%)
26	44	100	45
27	140	210	58

¹ Under nitrogen. ² Under argon.



Scheme 21. Network polymers prepared from PFPy. Conditions: a = 1,3,5-benzenetriol, DMF, 3.3 equiv. NaH, 65 °C, 16 h; b = phloroglucinol, DMF, 3.3 equiv. NaH, 65 °C, 16 h.

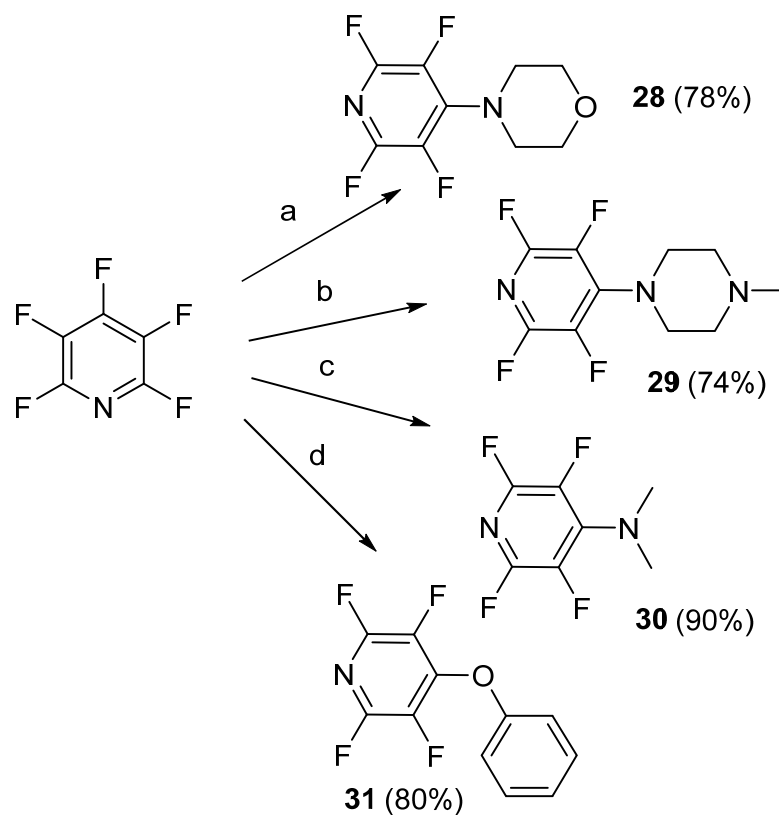
In June of 2020, Gomri et al. prepared new poly(ether pyridine) polymers for the capture of aromatic pollutants such as p-hydroxybenzoic acid, toluic acid, deisopropylatrazine, and 2,4,6-trichlorophenol, along with their halogenated derivatives, in contaminated water sources [73]. To synthesize the beginning monomers, SNAr was again utilized by adding nitrogen- and oxygen-based nucleophiles to PFPy (Scheme 22) [73]. In all cases, the nucleophile was added in the 4-position of PFPy, due to the stabilizing effect of the nitrogen carrying the extra but momentary negative charge, and resulted in the formation of pyridinium-based monomers.

Once the monomers were obtained, polycondensation reactions with bisphenol A (BPA) and isosorbide (IS) were performed to obtain the poly(ether pyridine) polymers. In order to perform the polycondensation, more forcing conditions were necessary. Both diols, BPA and IS, were heated to 140 °C and 160 °C, respectively (Scheme 23) [73].

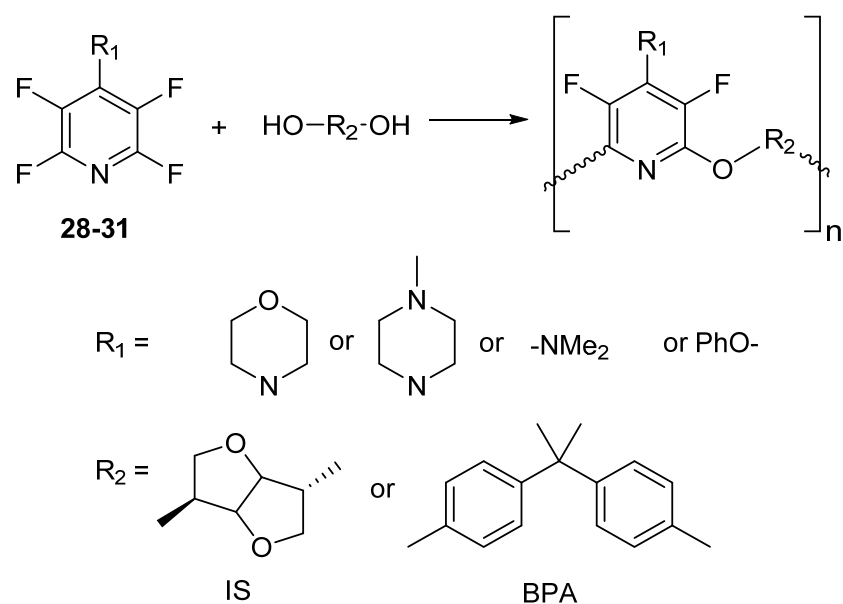
The resulting polymers were thermally characterized by DSC and TGA. The polymers had a T_g range of 102 to 206 °C and the 5% decomposition temperature ranged from 346 to 419 °C. The molecular weights determined by GPC did vary depending upon the monomers that were used. The largest molecular weight obtained with IS was evident with monomer 28, resulting in a number average molecular weight (M_n) of 21,330 g/mol. Were as for BPA, there were two monomers which performed decently in the polymerization, 28 and 30 having M_n of 105,700 g/mol and 25,170 g/mol, respectively. The dispersity for all the polymers ranged from 1.3 to 4.5 (see Table 8) [73].

The adsorption characteristics of the polymers were evaluated towards a variety of aromatic pollutants and their halogenated derivatives. Polymers based on IS showed improved adsorption capacity towards all the pollutants tested. Furthermore, polymers containing the morpholine-based monomer, 28, demonstrated enhanced absorption efficiencies greater than 90%. Thus, of all the polymers tested, 28/IS had the highest efficiency

towards the pollutants and their derivatives. The adsorption kinetics were found to fit well to a pseudo-second order mechanism, obeying a Freundlich isotherm model [73].



Scheme 22. Synthesis of pyridinium-based monomers, 28–31. Conditions: a = morpholine, NEt_3 , THF, RT, 48 h; b = N-methylpiperazine, NEt_3 , THF, RT, 48 h; c = dimethylamine, EtOH, 0 °C, 10 min; d = phenol, K_2CO_3 , DMF, RT, 2 h.



Scheme 23. Synthesis of poly(ether pyridine) polymers P1–P8. Conditions = K_2CO_3 , DMSO, 24 h.

Table 8. Selected thermal and molecular weight data obtained by Gomri et al. [73].

Polymer	Yield ¹ (%)	T _g ² (°C)	T _d ³ (°C)	M _n ⁴ (g/mol)	M _w ⁴ (g/mol)	D ⁴
28/BPA	98	146	419	105,700	291,700	2.7
28/IS	92	206	365	21,330	49,600	2.3
29/BPA	73	127	395	1961	2871	1.4
29/IS	79	170	363	1800	2454	1.3
30/BPA	95	124	408	25,170	112,000	4.5
30/IS	71	143	357	2743	4462	1.6
31/BPA	88	102	444	3523	10,590	4.1
31/IS	91	155	346	3017	6161	2

¹ Precipitation into MeOH, evaporation under vacuum at 60 °C. ² Obtained by DSC with heating at 10 °C/min. ³ Temperature at 5% mass loss. ⁴ Determined by GPC in CHCl₃ against PS standards.

In mid-2021, Stewart and co-workers were able to demonstrate that PFPy could be deployed in high-temperature silicon-based linear and network elastomers and oils [74]. As seen in the other examples above, the authors utilized the regioselective SNAr reaction to prepare a number of new PFPy-based monomers (Scheme 24) [74].

By reacting the terminal alkenes of these monomers with hydride-terminated polydimethylsiloxanes (H-PDMSs), linear silicon-based elastomers and oils were obtained. Interestingly, the polymer made from monomer **32** was found to be post-modifiable with 4-bromophenol to obtain a polymer with similar properties to that of one made from monomer **33** (Scheme 25) [74].

Additionally, compounds **18** and **19** that were previously reported, along with octadimethylhydrosilyl cubic siloxane (OctaSilane POSS), were utilized to form silicon-based networks (Figure 4) [69,74].

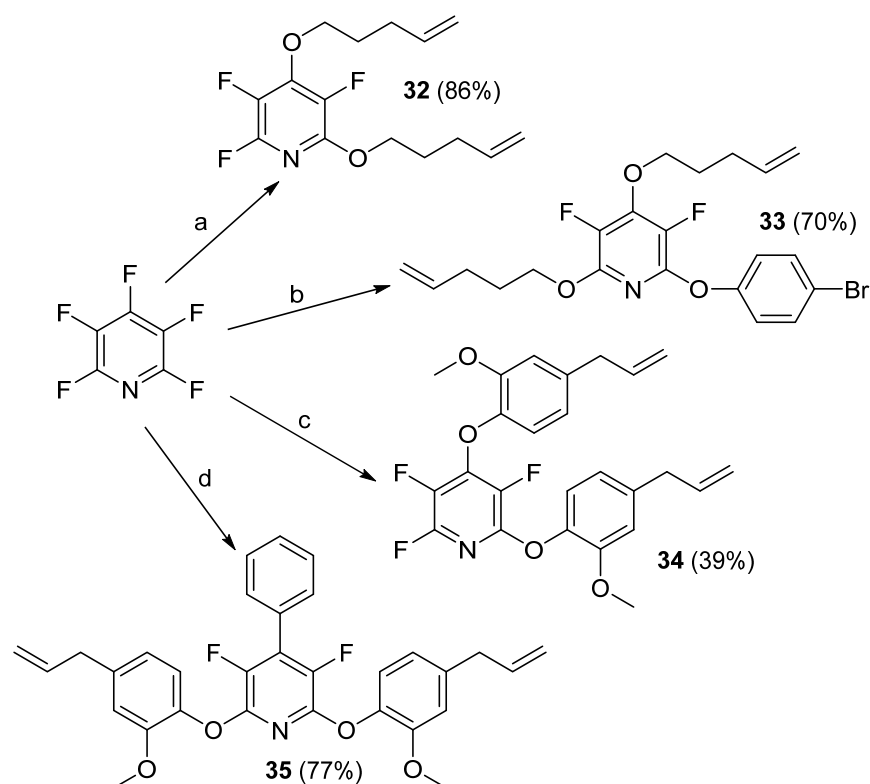
The potential application of this work focused on heat-shielding materials (HSMs) in rocket motor casings. These protective coatings not only have to withstand high heat upon re-entry but also extreme cold when deep in space. Thermal characterization showed that the linear polymers made with H-PDMSs (**poly32–35**) had T_gs ranging from −28 to −12 °C and T_ds ranging from 382 to 404 °C. Network polymers made from H-PDMS (**net18a–e** and **net19a–e**) were thermally stable with no onset of degradation up to 431 and 430 °C, and char yields as high as 43 and 62%, under inert pyrolysis conditions, respectively. In addition, aliphatic or aromatic content are programmable in order to control glass transition temperatures of the networks, allowing for T_gs ranging from −49 to 83 °C (Table 9) [74].

Later, in 2021, Houck et al. demonstrated the ability to prepare a variety of aryl ether-functionalized polymers using both pre- and post-functionalized approaches [75]. In order to accomplish this, the authors initially prepared three monomers capable of undergoing ring-opening metathesis polymerization (ROMP) (Scheme 26) [75]. Compounds **37** and **38** had been previously reported [76].

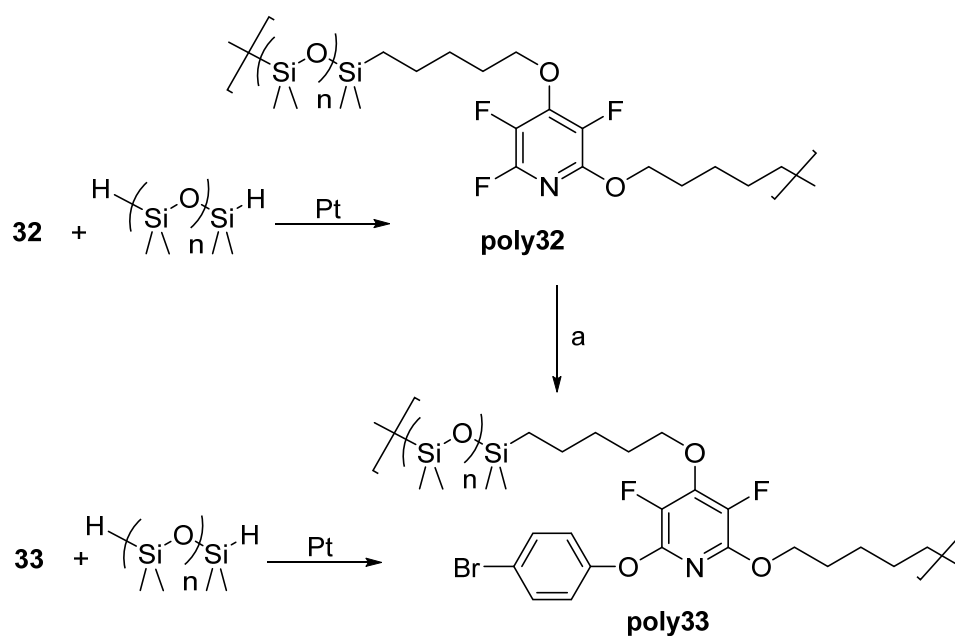
Monomer **36** was then either functionalized with ROH via SNAr or polymerized, to give **poly36**. **Poly36** could then post-functionalized with the ROH nucleophiles (Scheme 27) [75].

Similar methods were applied to monomer **37**, but only ROH = **a–f** were utilized. Interestingly, this is the first known report of chain growth polymers containing PFPy as a pendant group. Polymers prepared from **36** and **37** were characterized by GPC, TGA, and DSC (Table 10) [75].

Attempts to react monomer **38** with ROH resulted in a mixture of products and was attributed to the reversibility sometimes observed in the SNAr reaction at the 4-position [45,68]. The reversibility was also seen when attempts to post-functionalize **poly38** with the various ROH nucleophiles resulted in densely cross-linked polymer. DFT calculations, along with the experimental observations on the monomers utilized in this study, support that the reversibility of **38** could be attributed to having a small dihedral angle [75].



Scheme 24. Synthesis of PFPy-based monomers, **32–35**. Conditions: a = 4-penten-1-ol, Cs_2CO_3 , ACN, RT, 72 h; b = from **32**, 4-bromophenol, Cs_2CO_3 , DMF, 65 °C, 24 h; c = eugenol, Cs_2CO_3 , DMF, RT, 24 h; d = from **24**, eugenol, Cs_2CO_3 , DMF, RT, 24 h.



Scheme 25. Linear polymers prepared from **32**, **33**, and post-modification of **poly32**. Conditions: a = 4-bromophenol, Cs_2CO_3 , d_7 -DMF, 60 °C, 72–120 h.

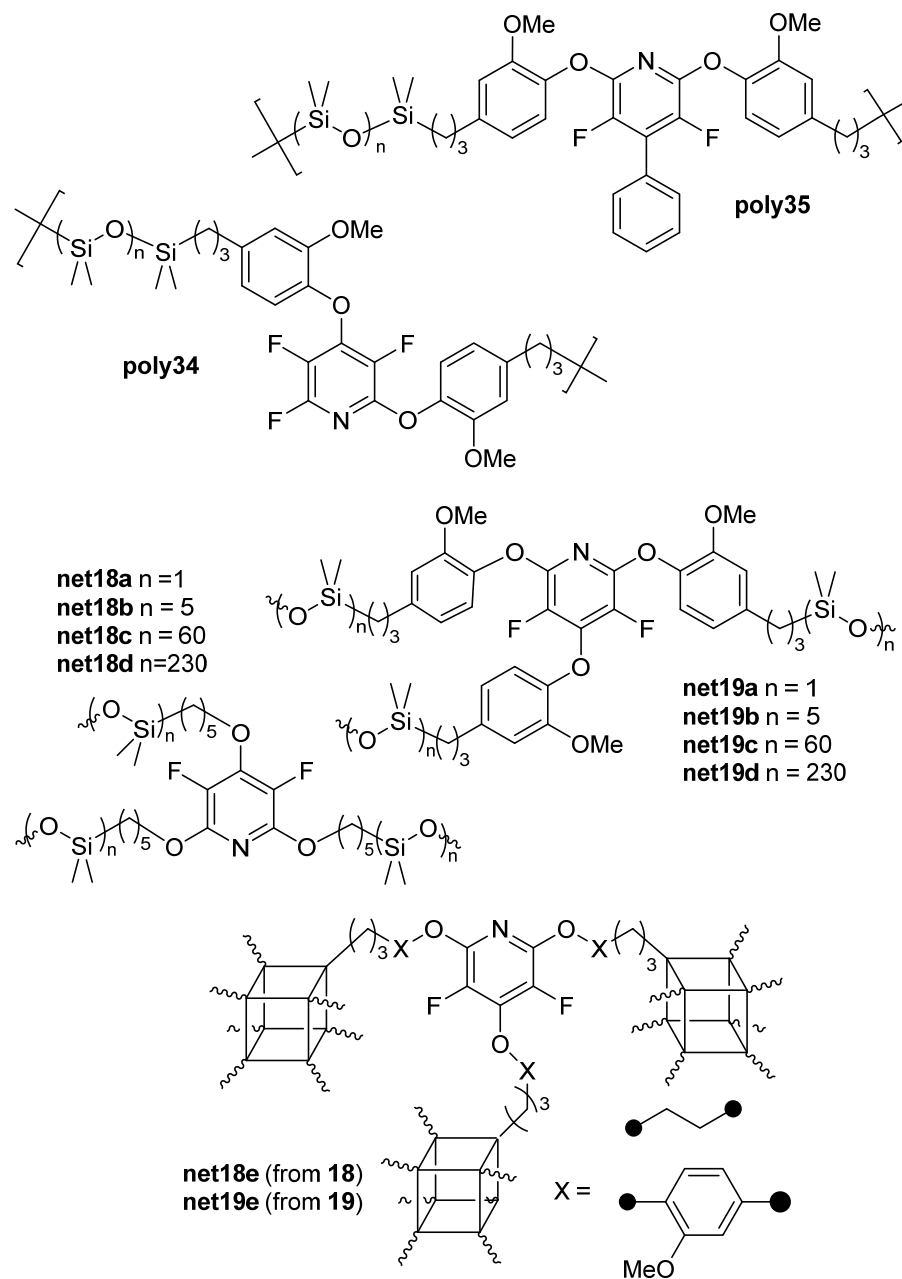


Figure 4. Linear polymers and networks prepared 18, 19, 34, and 35.

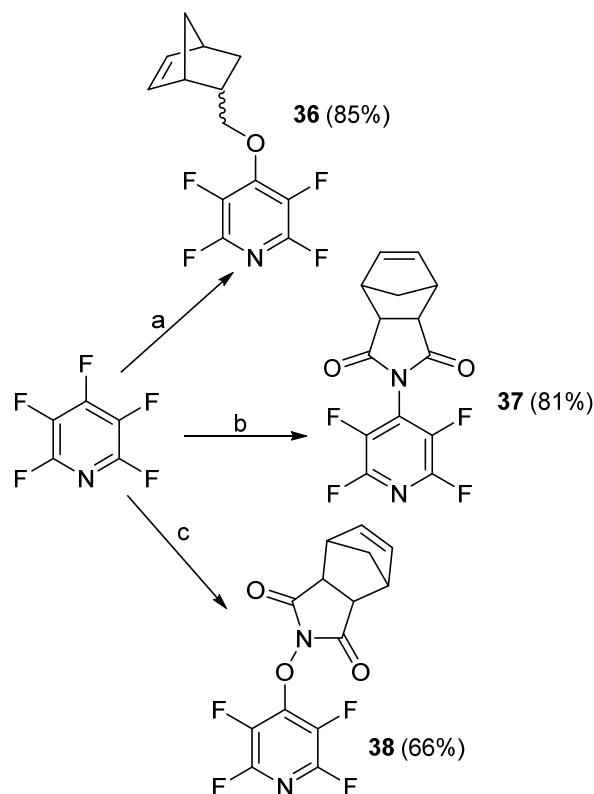
Table 9. Selected thermal data obtained by Stewart and co-workers [74].

Polymer/Network	T_g^1 (°C)	T_d^5 (°C)	Char Yield (%)
poly32	−25	360	3
poly33	−12	404	2
poly34	−26	388	14
poly35	−28	382	13
net18a ²	−45	378	9
net18b ²	−43	379	18
net18c ²	−49	409	43
net18d ²	− ³	418	33
net18e ²	28	407	49
net19a ²			
net19b ²	10	402	34

Table 9. Cont.

Polymer/Network	T_g ¹ (°C)	T_d ⁵ (°C)	Char Yield (%)
net19c ²		409	25
net19d ²	- ⁴	431	30
net19e ²	83	410	62

¹ DSC in nitrogen with heating at 5 °C/min determined on the third heating cycle. ² Data obtained after Soxhlet extraction. ³ Melt transition observed at -46 °C. ⁴ Melt transition observed at -38 °C. ⁵ MTGA onset in nitrogen with heating at 10 °C/min.



Scheme 26. ROMP monomers, **36–38**, prepared from PFPy. Conditions: a = bicyclo[2.2.1]hept-5-en-2-ylmethanol, Cs_2CO_3 , THF, RT, 16 h; b = (3aR,4S,7R,7aS)-3a,4,7,7a-tetrahydro-1H-4,7-methanoisindole-1,3(2H)-dione, Et_3N , DMF, RT, 24 h; c = (3aR,4S,7R,7aS)-2-hydroxy-3a,4,7,7a-tetrahydro-1H-4,7-methanoisindole-1,3(2H)-dione, K_2CO_3 , DMF, RT, 24 h.

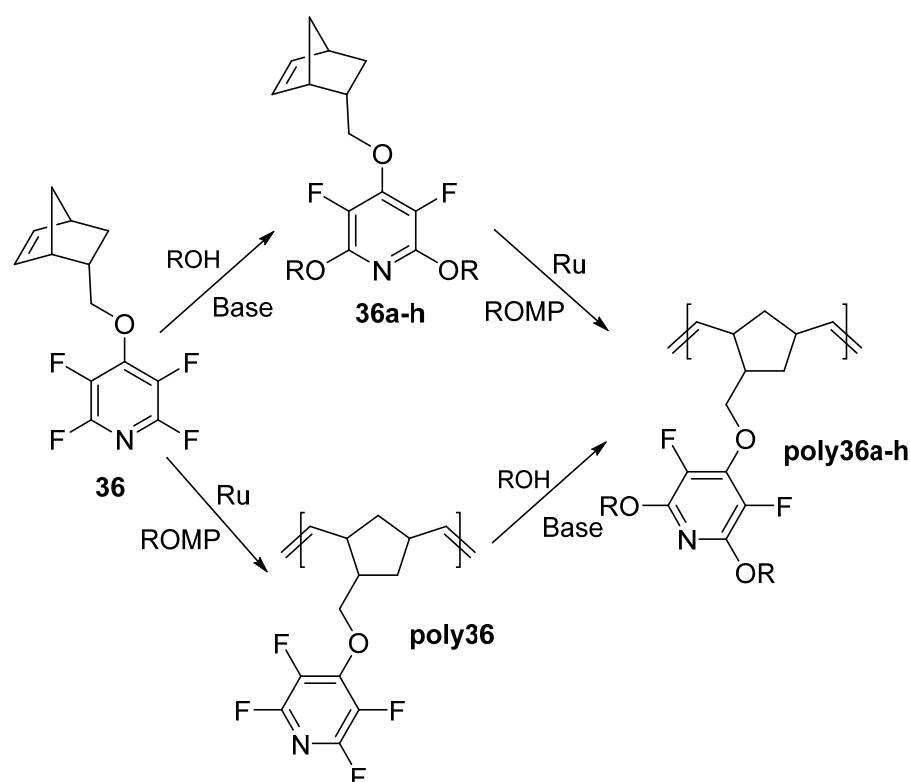
Table 10. Selected characterization data for the polymers prepared by the pre- and [post-] functionalization methods developed by Houck et al. [75].

Polymer	M_w ¹ (kDa)	\bar{D} ⁴	T_g ² (°C)	T_d ³ (°C)	Char Yield ⁴ (%)
poly36	332.7	2.5	6	127	8
poly36a	73.7 [128.9]	1.9 [1.4]	62	192	33
poly36b	112.1 [275.1]	2.1 [2.0]	62	247	28
poly36c	[228.1]	2.8		153	40
poly36d	32.1 [171.7]	2.1 [2.6]	138	312	9
poly36e	[54.9]	[2.2]	77	265	50
poly36f	[22.9]	[2.1]		181 (405) ⁵	45 (67) ⁵
poly36g	142.4	3.5	85	250	38
poly36h	[172.3]	[2.8]	81	293	29
poly37	217.0	2.1	227	229	30
poly37a	55.4 [28.2]	1.9 [2.0]	186	392	29
poly37b	192.7 [55.5]	2.0 [1.8]	175	385	35

Table 10. Cont.

Polymer	M_w ¹ (kDa)	D ⁴	T_g ² (°C)	T_d ³ (°C)	Char Yield ⁴ (%)
poly37c	2.3	2.8	100	376	58
poly37d	69.9	1.9	190	368	26
poly37e	127.0	3.2		233	52
Poly37f	[73.3]	[1.8]		62 (355) ⁵	49 (60) ⁵

¹ Determined by GPC in THF against PS standards. ² DSC in nitrogen with heating at 5 °C/min, determined on the third heating cycle. ³ TGA onset in nitrogen with heating at 10 °C/min. ⁴ TGA at 900 °C in nitrogen. ⁵ Values observed as the second scan after cure by DSC.



Scheme 27. Monomer functionalization and polymer post-functionalization method applied to 36. ROH: a = phenol, b = 4-methoxyphenol, c = eugenol, d = 4-bromophenol, e = 4-nitrophenol, f = propargyl alcohol, g = 4-methoxyphenol and 4-bromophenol, h = 2-naphtanlenol.

5. Conclusions and Perspective

Organofluorine compounds are highly sought after materials because of their unique chemistries and desired properties. With its commercial availability and distinctive reactivity, PFPy is no exception and it has found use in a number of advanced applications. Despite this, it is the authors' perspective that the use of PFPy in obtaining fluorinated polymers and materials is still gaining momentum. Although its synthesis was first reported in the 1960s, PFPy was not utilized for preparing a fluorinated polymer until nearly 20 years later. To the authors' knowledge, there are only about 15 peer-reviewed publications with PFPy being employed to make fluorinated networks or fluoropolymers, with the majority of these works being published within the last decade. In all accounts, PFPy is utilized via S_NAr to craft the fluorinated network material or polymer, and there is only one example where PFPy is used to fluorinate an existing polymer. Additionally, the majority of these fluoropolymers and networks employ PFPy in the backbone of the polymer versus a pendant group. Lastly, most of these advanced fluorinated materials are obtained through step-growth polymerization techniques, which might be attributed to the propensity of PFPy to react with nucleophiles.

Author Contributions: Conceptualization—A.R.J.; literature search—R.G., I.G., S.T.I. and A.R.J.; writing—original draft preparation—R.G., I.G., S.T.I., C.M.F. and A.R.J.; writing—review and editing—A.R.J.; supervision—A.R.J.; funding acquisition—S.T.I. All authors have read and agreed to the published version of the manuscript.

Funding: S.T.I. and A.R.J. acknowledge financial support for the APC from the Air Force Office of Scientific Research (AFOSR). This work by C.M.F. was accomplished during his tenure as part of the U.S. Air Force Research Lab Summer Faculty Fellowship Program (SFFP) funded by AFOSR.

Institutional Review Board Statement: PA#: USAFA-DF-2022-35, DISTRIBUTION STATEMENT A: Approved for public release: distribution unlimited. **DISCLAIMER:** The views expressed in this article, book, or presentation are those of the author and do not necessarily reflect the official policy or position of the United States Air Force Academy, the Air Force, the Department of Defense, or the U.S. Government.

Informed Consent Statement: Not applicable.

Data Availability Statement: Not applicable.

Acknowledgments: The authors acknowledge AFOSR for financially supporting this work.

Conflicts of Interest: The authors declare no conflict of interest.

References

1. Clark, C.H.D. Atomic radius of fluorine. *Nature* **1934**, *134*, 99–100. [[CrossRef](#)]
2. Smart, B.E. Characteristics of the C-F Systems. In *Organofluorine Chemistry—Principles and Commercial Applications*; Banks, R.E., Smart, B.E., Tatlow, J.C., Eds.; Plenum Press: New York, NY, USA; London, UK, 1994; pp. 57–82, ISBN 978–1-4899-1202-2.
3. Tressaud, A. 2—Fluorine, a key element for the 21st century. In *Fluorine*; Tressaud, A., Ed.; Elsevier: Amsterdam, The Netherlands, 2019; Volume 5, pp. 77–150, ISBN 978-0-12-812990-6.
4. Cosco, D.; Fattal, E.; Fresta, M.; Tsapis, N. Perfluorocarbon-loaded micro and nanosystems for medical imaging: A state of the art. *J. Fluor. Chem.* **2015**, *171*, 18–26. [[CrossRef](#)]
5. Hequet, E.; Henoumont, C.; Muller, R.N.; Laurent, S. Fluorinated MRI contrast agents and their versatile applications in the biomedical field. *Future Med. Chem.* **2019**, *11*, 1157–1175. [[CrossRef](#)] [[PubMed](#)]
6. Inoue, M.; Sumii, Y.; Shibata, N. Contribution of Organofluorine Compounds to Pharmaceuticals. *ACS Omega* **2020**, *5*, 10633–10640. [[CrossRef](#)] [[PubMed](#)]
7. Ogawa, Y.; Tokunaga, E.; Kobayashi, O.; Hirai, K.; Shibata, N. Current Contributions of Organofluorine Compounds to the Agrochemical Industry. *iScience* **2020**, *23*, 101467. [[CrossRef](#)] [[PubMed](#)]
8. Smith, D.W., Jr.; Iacono, S.T.; Iyer, S.S. (Eds.) *Handbook of Fluoropolymer Science and Technology*; John Wiley & Sons, Inc.: Hoboken, NJ, USA, 2014; ISBN 978-0-470-07993-5.
9. Okazoe, T. Overview on the history of organofluorine chemistry from the viewpoint of material industry. *Proc. Jpn. Acad. B-Phys.* **2009**, *85*, 276–289. [[CrossRef](#)]
10. Okazoe, T. Development of the “PERFECT” direct fluorination method and its industrial applications. *J. Fluor. Chem.* **2015**, *174*, 120–131. [[CrossRef](#)]
11. Daglar, O.; Cakmakci, E.; Gunay, U.S.; Hizal, G.; Tunca, U.; Durmaz, H. A Straightforward Method for Fluorinated Polythioether Synthesis. *Macromolecules* **2020**, *53*, 2965–2975. [[CrossRef](#)]
12. Brittain, W.D.G.; Cobb, S.L. Tetrafluoropyridyl (TFP): A general phenol protecting group readily cleaved under mild conditions. *Org. Biomol. Chem.* **2019**, *17*, 2110–2115. [[CrossRef](#)]
13. Liljenberg, M.; Brinck, T.; Herschend, B.; Rein, T.; Tomasi, S.; Svensson, M. Predicting Regioselectivity in Nucleophilic Aromatic Substitution. *J. Org. Chem.* **2012**, *77*, 3262–3269. [[CrossRef](#)]
14. Darehkordi, A.; Ramezani, M.; Rahmani, F.; Ramezani, M. Design, Synthesis and Evaluation of Antibacterial Effects of a New Class of Piperazinylquinolone Derivatives. *J. Heterocycl. Chem.* **2016**, *53*, 89–94. [[CrossRef](#)]
15. Yang, W.-Y.; Breiner, B.; Kovalenko, S.V.; Ben, C.; Singh, M.; LeGrand, S.N.; Sang, Q.-X.A.; Strouse, G.F.; Copland, J.A.; Alabugin, I.V. C-Lysine Conjugates: pH-Controlled Light-Activated Reagents for Efficient Double-Stranded DNA Cleavage with Implications for Cancer Therapy. *J. Am. Chem. Soc.* **2009**, *131*, 11458–11470. [[CrossRef](#)] [[PubMed](#)]
16. Gimenez, D.; Mooney, C.A.; Dose, A.; Sandford, G.; Coxon, C.R.; Cobb, S.L. The application of perfluoroheteroaromatic reagents in the preparation of modified peptide systems. *Org. Biomol. Chem.* **2017**, *15*, 4086–4095. [[CrossRef](#)] [[PubMed](#)]
17. Sandford, G. Macrocycles from Perhalogenated Heterocycles. *Chem. Eur. J.* **2003**, *9*, 1464–1469. [[CrossRef](#)]
18. Trawny, D.; Kunz, V.; Reissig, H.-U. Modular Syntheses of Star-Shaped Pyridine, Bipyridine, and Terpyridine Derivatives by Employing Sonogashira Reactions. *Eur. J. Org. Chem.* **2014**, *2014*, 6295–6302. [[CrossRef](#)]
19. Gutov, A.V.; Rusanov, E.B.; Ryabitskii, A.B.; Chernega, A.N. Octafluoro-4,4′-bipyridine and its derivatives: Synthesis, molecular and crystal structure. *J. Fluor. Chem.* **2010**, *131*, 278–281. [[CrossRef](#)]
20. Banks, R.E.; Ginsberg, A.E.; Haszeldine, R.N. Pentafluoropyridine. *Proc. Chem. Soc.* **1960**, 211. [[CrossRef](#)]

21. Burdon, J.; Gilman, D.J.; Patrick, C.R.; Stacey, M.; Tatlow, J.C. Pentafluoropyridine. *Nature* **1960**, *186*, 231–232. [CrossRef]
22. Banks, R.E.; Ginsberg, A.E.; Haszeldine, R.N. 338. Heterocyclic polyfluoro-compounds. Part I. Pentafluoropyridine. *J. Chem. Soc.* **1961**, 1740–1743. [CrossRef]
23. Haszeldine, R.N.; Banks, R.E.; Ginsberg, A.E. Perfluorinated Aromatic Heterocyclic Compounds. UK Patent GB 980,248, 13 January 1965.
24. Haszeldine, R.N.; Nyman, F. Perfluoroalkyl derivatives of sulfur. V. α,α -Difluoro- α -(trifluorothio)acetic acid. *J. Chem. Soc.* **1956**, 2684–2689. [CrossRef]
25. Chambers, R.D.; Hutchinson, J.; Musgrave, W.K.R. Pentafluoro- and chlorofluoropyridines. *Proc. Chem. Soc.* **1964**, 83. [CrossRef]
26. Chambers, R.D.; Hutchinson, J.; Musgrave, W.K.R. Fluoropyridines and Their Derivatives. U.S. Patent BE 660, 873, 10 March 1965.
27. Chambers, R.D.; Hutchinson, J.; Rodgerson Musgrave, W.K. Fluorinated Pyridines. UK Patent GB 1,107,881, 27 March 1968.
28. Banks, R.E.; Haszeldine, R.N.; Latham, J.V.; Young, I.M. Polyfluoropyridines. *Chem. Ind.* **1964**, 20, 835.
29. Banks, R.E.; Haszeldine, R.N.; Latham, J.V.; Young, I.M. 95. Heterocyclic polyfluoro-compounds. Part VI. Preparation of pentafluoropyridine and chlorofluoropyridines from pentachloropyridine. *J. Chem. Soc.* **1965**, 594–597. [CrossRef]
30. Sell, W.J.; Dootson, F.W. XLV.—The chlorine derivatives of pyridine. Part I. *J. Chem. Soc. Trans.* **1898**, 73, 432–441. [CrossRef]
31. Banks, R.E.; Barlow, M.G.; Mamaghani, M. Vacuum pyrolysis of 4-(dichloroamino)tetrafluoropyridine and related compounds. *J. Fluor. Chem.* **1981**, *17*, 197–203. [CrossRef]
32. Coe, P.L.; Sleight, J.H. Highly fluorinated heterocycles part XV [1]. The metal catalysed defluorinative rearrangement of polyfluorinated pyrrolidines to polyfluoropyridines. *J. Fluor. Chem.* **1981**, *17*, 403–407. [CrossRef]
33. Plevy, R.G.; Rendell, R.W.; Tatlow, J.C. Fluorinations with complex metal fluorides. Part 6 [1] fluorination of yridine and related compounds with caesium tetrafluorocobaltate(III)[2]. *J. Fluor. Chem.* **1982**, *21*, 159–169. [CrossRef]
34. Bardin, V.V.; Trukhin, D.V.; Adonin, N.Y.; Starichenko, V.F. Dehalogenative aromatization of perchlorofluoroalicyclic compounds C₆Cl₆F₆, C₁₀Cl₈F₈ and C₅Cl₄F₅N in the vapour phase or in solution. *J. Fluor. Chem.* **2004**, *125*, 1431–1435. [CrossRef]
35. SciFinder. Available online: <https://scifinder.cas.org/scifinder> (accessed on 28 November 2021).
36. Amii, H.; Uneyama, K. C–F Bond Activation in Organic Synthesis. *Chem. Rev.* **2009**, *109*, 2119–2183. [CrossRef]
37. Lipilin, D.L.; Frumkin, A.E.; Tyurin, A.Y.; Levin, V.V.; Dilman, A.D. Photoredox Catalyzed Dealkylative Aromatic Halogen Substitution with Tertiary Amines. *Molecules* **2021**, *26*, 3323. [CrossRef] [PubMed]
38. Zubkov, M.O.; Kosobokov, M.D.; Levin, V.V.; Kokorekin, V.A.; Korlyukov, A.A.; Hu, J.; Dilman, A.D. A novel photoredox-active group for the generation of fluorinated radicals from difluorostyrenes. *Chem. Sci.* **2020**, *11*, 737–741. [CrossRef] [PubMed]
39. McKay, D.; Riddlestone, I.M.; Macgregor, S.A.; Mahon, M.F.; Whittlesey, M.K. Mechanistic Study of Ru-NHC-Catalyzed Hydrodefluorination of Fluoropyridines: The Influence of the NHC on the Regioselectivity of C–F Activation and Chemoselectivity of C–F versus C–H Bond Cleavage. *ACS Catal.* **2015**, *5*, 776–787. [CrossRef]
40. Arévalo, A.; Tlahuext-Aca, A.; Flores-Alamo, M.; García, J.J. On the Catalytic Hydrodefluorination of Fluoroaromatics Using Nickel Complexes: The True Role of the Phosphine. *J. Am. Chem. Soc.* **2014**, *136*, 4634–4639. [CrossRef] [PubMed]
41. Wielgat, J.; Domagala, Z. Reaction of pentafluoropyridine with bifunctional nucleophiles. *Rocz. Chem.* **1975**, *49*, 1039–1041.
42. Neumann, C.N.; Hooker, J.M.; Ritter, T. Concerted nucleophilic aromatic substitution with 19F[−] and 18F[−]. *Nature* **2016**, *534*, 369–373. [CrossRef]
43. Sandford, G. Perfluoroheteroaromatic Chemistry: Multifunctional Systems from Perfluorinated Heterocycles by Nucleophilic Aromatic Substitution Processes. In *Halogenated Heterocycles: Synthesis Applications and Environment*; Iskra, J., Ed.; Springer: Berlin/Heidelberg, Germany, 2012; pp. 1–31, ISBN 978-3-642-43950-6.
44. Vlasov, V.M.; Aksenov, V.V.; Rodionov, P.P.; Beregovaya, I.V.; Shchegoleva, L.N. Unusual Lability of Pentafluorophenoxy Group in Reactions of Potassium Aroxides with Pentafluoropyridine. *Russ. J. Org. Chem.* **2002**, *38*, 115–125. [CrossRef]
45. Fuhrer, T.J.; Houck, M.; Corley, C.A.; Iacono, S.T. Theoretical Explanation of Reaction Site Selectivity in the Addition of a Phenoxy Group to Perfluoropyridine. *J. Phys. Chem. A* **2019**, *123*, 9450–9455. [CrossRef]
46. Murray, C.B.; Sandford, G.; Korn, S.R.; Yufit, D.S.; Howard, J.A.K. New fluoride ion reagent from pentafluoropyridine. *J. Fluor. Chem.* **2005**, *126*, 569–574. [CrossRef]
47. Brittain, W.D.G.; Cobb, S.L. Carboxylic Acid Deoxyfluorination and One-Pot Amide Bond Formation Using Pentafluoropyridine (PFP). *Org. Lett.* **2021**, *23*, 5793–5798. [CrossRef]
48. Senaweera, S.M.; Singh, A.; Weaver, J.D. Photocatalytic Hydrodefluorination: Facile Access to Partially Fluorinated Aromatics. *J. Am. Chem. Soc.* **2014**, *136*, 3002–3005. [CrossRef]
49. Froese, R.D.J.; Whiteker, G.T.; Peterson, T.H.; Arriola, D.J.; Renga, J.M.; Shearer, J.W. Computational and Experimental Studies of Regioselective S_NAr Halide Exchange (Halx) Reactions of Pentachloropyridine. *J. Org. Chem.* **2016**, *81*, 10672–10682. [CrossRef] [PubMed]
50. Plunkett, R.J. Tetrafluoroethylene Polymers. U.S. Patent 2,230,654, 4 February 1941.
51. Feiring, A.E. Fluoroplastics. In *Organofluorine Chemistry: Principles and Commercial Applications*; Banks, R.E., Smart, B.E., Tatlow, J.C., Eds.; Springer: Boston, MA, USA, 1994; pp. 339–372, ISBN 978-1-4899-1202-2.
52. Améduri, B. The Promising Future of Fluoropolymers. *Macromol. Chem. Phys.* **2020**, *221*, 1900573. [CrossRef]
53. Scheirs, J. *Modern Fluoropolymers: High Performance Polymers for Diverse Applications*; Scheirs, J., Ed.; Wiley: New York, NY, USA, 1997; ISBN 978-0-471-97055-2.

54. Cardoso, V.F.; Correia, D.M.; Ribeiro, C.; Fernandes, M.M.; Lanceros-Méndez, S. Fluorinated Polymers as Smart Materials for Advanced Biomedical Applications. *Polymers* **2018**, *10*, 161. [[CrossRef](#)]
55. Belov, N.A.; Alentiev, A.Y.; Bogdanova, Y.G.; Vdovichenko, A.Y.; Pashkevich, D.S. Direct Fluorination as Method of Improvement of Operational Properties of Polymeric Materials. *Polymers* **2020**, *12*, 2836. [[CrossRef](#)] [[PubMed](#)]
56. Johncock, P.; Hewins, M.A.H.; Cunliffe, A.V. Polyfluoroethers from 1,1,5,5-tetrahydro-1,5-pentanediol and polyfluoroaromatic and polyfluoroheteroaromatic compounds. *J. Polym. Sci. Polym. Chem. Ed.* **1976**, *14*, 365–378. [[CrossRef](#)]
57. Cook, J.D.; Wakefield, B.J. Polyhalogenoaromatic compounds. Part VIII. Reaction of aryl-lithium compounds with tetrachloro-4-methoxypyridine, and of aryl-substituted polychloropyridines with n-butyl-lithium. *J. Chem. Soc. C* **1969**, 2376–2378. [[CrossRef](#)]
58. Chambers, R.D.; Hutchinson, J.; Musgrave, W.K.R. 722. Polyfluoro-heterocyclic compounds. Part II. Nucleophilic substitution in pentafluoropyridine. *J. Chem. Soc.* **1964**, 3736–3739. [[CrossRef](#)]
59. Banks, R.E.; Burgess, J.E.; Cheng, W.M.; Haszeldine, R.N. 93. Heterocyclic polyfluoro-compounds. Part IV. Nucleophilic substitution in pentafluoropyridine: The preparation and properties of some 4-substituted 2,3,5,6-tetrafluoropyridines. *J. Chem. Soc.* **1965**, 575–581. [[CrossRef](#)]
60. Banks, R.E.; Tsioliopoulos, E. Polymeric analogues of electrophilic fluorinating agents of the N-F class. *J. Fluor. Chem.* **1986**, *34*, 281–285. [[CrossRef](#)]
61. Seyb, C.; Kerres, J. Novel partially fluorinated sulfonated poly(arylenethioether)s and poly(aryleneether)s prepared from octafluorotoluene and pentafluoropyridine, and their blends with PBI-Celazol. *Eur. Polym. J.* **2013**, *49*, 518–531. [[CrossRef](#)]
62. Vaganova, T.A.; Kusov, S.Z.; Rodionov, V.I.; Shundrina, I.K.; Malykhin, E.V. Selective mono- and diamination of polyfluorinated benzenes and pyridines with liquid ammonia. *Russ. Chem. Bull.* **2007**, *56*, 2239–2246. [[CrossRef](#)]
63. Kusov, S.Z.; Rodionov, V.I.; Vaganova, T.A.; Shundrina, I.K.; Malykhin, E.V. Direct di- and triamination of polyfluoropyridines in anhydrous ammonia. *J. Fluor. Chem.* **2009**, *130*, 461–465. [[CrossRef](#)]
64. Vaganova, T.A.; Shundrina, I.K.; Kusov, S.Z.; Rodionov, V.I.; Malykhin, E.V. Synthesis and characterization of novel fluorinated pyridine-based polyimides. *J. Fluor. Chem.* **2013**, *149*, 57–64. [[CrossRef](#)]
65. Chapyshev, S.V. Di- and triazidation of 3-chlorotetrafluoropyridine. *J. Fluor. Chem.* **2011**, *132*, 991–994. [[CrossRef](#)]
66. Nedel'ko, V.V.; Chukanov, N.V.; Korsunskiy, B.L.; Larikova, T.S.; Chapyshev, S.V.; Zakharov, V.V. Kinetics of the Thermal Decomposition of 2,4,6-Triazido-3,5-Difluoropyridine. *Russ. J. Phys. Chem. B* **2018**, *12*, 997–1002. [[CrossRef](#)]
67. Yu, T.; Xue, Z.; Zhao, X.; Chen, W.; Mu, T. Green synthesis of porous β -cyclodextrin polymers for rapid and efficient removal of organic pollutants and heavy metal ions from water. *New J. Chem.* **2018**, *42*, 16154–16161. [[CrossRef](#)]
68. Corley, C.A.; Kobra, K.; Peloquin, A.J.; Salmon, K.; Gumireddy, L.; Knoerzer, T.A.; McMillen, C.D.; Pennington, W.T.; Schoffstall, A.M.; Iacono, S.T. Utilizing the regioselectivity of perfluoropyridine towards the preparation of phenoxyacetylene precursors for partially fluorinated polymers of diverse architecture. *J. Fluor. Chem.* **2019**, *228*, 109409. [[CrossRef](#)]
69. Moore, L.M.J.; Greeson, K.T.; Stewart, K.A.; Kure, D.A.; Corley, C.A.; Jennings, A.R.; Iacono, S.T.; Ghiassi, K.B. Perfluoropyridine as a Scaffold for Semifluorinated Thiol-ene Networks with Readily Tunable Thermal Properties. *Macromol. Chem. Phys.* **2020**, *221*, 2000100. [[CrossRef](#)]
70. Houck, M.B.; Brown, L.C.; Lambeth, R.H.; Iacono, S.T. Exploiting the Site Selectivity of Perfluoropyridine for Facile Access to Densified Polyarylene Networks for Carbon-Rich Materials. *ACS Macro Lett.* **2020**, *9*, 964–968. [[CrossRef](#)]
71. Eismeier, S.; Peloquin, A.J.; Stewart, K.A.; Corley, C.A.; Iacono, S.T. Pyridine-functionalized linear and network step-growth fluoropolymers. *J. Fluor. Chem.* **2020**, *238*, 109631. [[CrossRef](#)]
72. Sun, Y.; Sun, H.; Jia, J.; Du, A.; Li, X. Transition-Metal-Free Synthesis of Fluorinated Arenes from Perfluorinated Arenes Coupled with Grignard Reagents. *Organometallics* **2014**, *33*, 1079–1081. [[CrossRef](#)]
73. Gomri, M.; Abderrazak, H.; Chabbah, T.; Souissi, R.; Saint-Martin, P.; Casabianca, H.; Chatti, S.; Mercier, R.; Errachid, A.; Hammami, M.; et al. Adsorption characteristics of aromatic pollutants and their halogenated derivatives on bio-based poly(ether-pyridine)s. *J. Environ. Chem. Eng.* **2020**, *8*, 104333. [[CrossRef](#)]
74. Stewart, K.A.; Shuster, D.; Leising, M.; Coolidge, I.; Lee, E.; Stevens, C.; Peloquin, A.J.; Kure, D.; Jennings, A.R.; Iacono, S.T. Synthesis, Characterization, and Thermal Properties of Fluoropyridyl-Functionalized Siloxanes of Diverse Polymeric Architectures. *Macromolecules* **2021**, *54*, 4871–4879. [[CrossRef](#)]
75. Houck, M.B.; Fuhrer, T.J.; Phelps, C.R.; Brown, L.C.; Iacono, S.T. Toward Taming the Chemical Reversibility of Perfluoropyridine through Molecular Design with Applications to Pre- and Postmodifiable Polymer Architectures. *Macromolecules* **2021**, *54*, 5586–5594. [[CrossRef](#)]
76. Peloquin, A.J.; Balaich, G.J.; Iacono, S.T. Syntheses, crystal structures and Hirshfeld surface analyses of (3aR,4S,7R,7aS)-2-(perfluoro-pyridin-4-yl)-3a,4,7,7a-tetra-hydro-4,7-methano-iso-indole-1,3-dione and (3aR,4S,7R,7aS)-2-[(perfluoro-pyridin-4-yl)-oxy]-3a,4,7,7a-tetra-hydro-4,7-methano-iso-indole-1,3-dione. *Acta Crystallogr. E* **2019**, *75*, 1153–1157. [[CrossRef](#)]